

Possible origins, mountainous microendemism and elevational range distribution in *Stumpffia* frogs (Microhylidae: Cophylinae) on Montagne d'Ambre in North Madagascar

N. Joris Fleck^{1,2,3,4}, Alice Petzold^{5,6}, Andolalao Rakotoarison^{7,8}, Miguel Vences⁹, Mark D. Scherz²

1 Institute for Biology, Leipzig University, Talstraße 33, 04103 Leipzig, Germany

2 Natural History Museum Denmark, Universitetsparken 15, 2100 Copenhagen Ø, Denmark

3 Zoologische Staatssammlung München (ZSM-SNSB), Münchhausenstr. 21, 81247 Munich, Germany

4 Biozentrum, Ludwig-Maximilians-Universität München, Großhaderner Straße 2–4, 82152 Planegg-Martinsried, Germany

5 Institute of Biochemistry and Biology, University of Potsdam, Karl-Liebknecht-Str. 24–25, 14476 Potsdam, Germany

6 Museum für Naturkunde, Leibniz Institute for Evolution and Biodiversity Science, Invalidenstr. 43, 10115 Berlin, Germany

7 School for International Training, VN 41A Bis Ambohitsoa, 101 Antananarivo, Madagascar

8 Mention Environnement, Université de l'Itasy, Faliarivo Ambohitanaerana, 118 Soavinandriana Itasy, Madagascar

9 Zoologisches Institut, Technische Universität Braunschweig, Mendelsohnstr. 4, 38106 Braunschweig, Germany

Corresponding author: Mark D. Scherz (mark.scherz@gmail.com)

Academic editor Deepak Veerappan | **Received** 11 August 2025 | **Accepted** 30 October 2025 | **Published** 21 January 2026

Citation: Fleck NJ, Petzold A, Rakotoarison A, Vences M, Scherz MD (2026) Possible origins, mountainous microendemism and elevational range distribution in *Stumpffia* frogs (Microhylidae: Cophylinae) on Montagne d'Ambre in North Madagascar. Vertebrate Zoology 76: 51–72. <https://doi.org/10.3897/vz.76.e166419>

Abstract

The role of regional diversification versus the effect of migration in generating local species assemblages remains poorly known. Here, we contribute to the understanding of the role of colonisation and in situ diversification by studying an assemblage of miniaturised microhylid frogs of the genus *Stumpffia* Boettger, 1881, of which six species have been known to occur on Montagne d'Ambre, a volcanic mountain in the north of Madagascar. These six species are distributed over different, partly overlapping elevational levels. We examined this assemblage based on molecular data (16S mtDNA and Rag1 nDNA), new data on the elevational distribution among local *Stumpffia* species, and differences in advertisement calls. Our results revealed several genetic lineages constituting distinct species, including another species record for the mountain, *S. mamilika* Rakotoarison et al., 2017, as well as the new candidate species *Stumpffia* sp. aff. *angeluci*. This brings the total number of described species known to occur on the mountain to seven, four of which are micro-endemic. Our data indicate that one clade, consisting of four species, has arisen in situ as a microendemic radiation. We discuss alternative evolutionary scenarios for the biogeographic origin of the observed *Stumpffia* species.

Keywords

Amphibia, Anura, bioacoustics, biogeography, in situ diversification, mountain diversification, *Stumpffia mamilika*, systematics, taxonomy

Introduction

Mountains have been reported to function as speciation pumps in various study systems (Hall 2005; Wollenberg et al. 2008; Lei et al. 2015; Steinbauer et al. 2016; Oliver et al. 2017; García-Rodríguez et al. 2021), and although they make up less than 15% of all land surfaces, they harbour 80% of the world's terrestrial biodiversity (García-Rodríguez et al. 2021). The extent of mountain biodiversity may be influenced positively by climatic and geological factors such as high mean annual temperature, high precipitation, a complex relief, and high soil type diversity (Antonelli et al. 2018). Furthermore, the proportion of (micro-) endemic species has been found to increase with higher elevation (Steinbauer et al. 2016; Oliver et al. 2017, Scherz et al. 2023).

The assemblage of species on a given mountain may be the result of colonisation and/or in situ diversification. For organisms without airborne life stages, colonisation is mostly limited to terrestrial routes, and consequently the highest point of opportunity for colonisation is the highest point of connectivity with the rest of the landscape (Knox 2004). The geographical context of a mountain shapes the opportunities for colonisation (Rahbek et al. 2019), and the ecological challenges faced by the assemblage of species that inhabit it (Antonelli et al. 2018): Isolated mountains surrounded by lowlands must be colonised from the lowlands, which can lead to a profile of phylogenetically younger lineages with increasing elevation (e.g., Oliver et al. 2017). In contrast, mountains that are part of mountain ranges and retain (or had at some point in their history) a connection to other nearby mountains, may be/have been colonised through dispersal paths at higher elevations (i.e., at the elevation of the connection between two mountains) (e.g., Knox 2004; Hofmann et al. 2017; Graham et al. 2023). This difference influences the extent of ecological challenge associated with the colonisation of a new mountain; climate fluctuations notwithstanding, terrestrial organisms colonising isolated mountains must initially live in the low elevation microclimate, before adapting to up-slope conditions (Oliver et al. 2017). This constitutes a much more extreme transition than an organism colonising at intermediate elevation via a ridge (Antonelli et al. 2018). However, fluctuations in climate on a geological time scale may shift the relative position, connectivity or fragmentation of patches of ecozones across the mountain, resulting in a flickering connectivity system (Flantua et al. 2019) and, thus, driving speciation (e.g., Hazzi and Wood 2025). Highly dynamic spatial shifts in mountainous vegetation zonation and plant biodiversity have been reported especially from the Pleistocene (Flantua and Hooghiemstra 2018; Flantua et al. 2019; Muellner-Riehl 2019; Muellner-Riehl et al. 2019), suggesting similar dynamics in zoological species assemblages.

Once on a given mountain, lineages may diverge from the initial point of colonization, and further diversify in situ. This can occur through a variety of mechanisms. The way we think about speciation has recently shifted

from focusing on a spatial context (allopatry vs. sympatry; Mayr 1942) towards the actual drivers of diversification, such as drift, sexual selection, or ecological selection (Nosil 2012), all of which can occur in any spatial/geographical contexts (i.e., sympatric/allopatric/parapatric settings; Nosil 2012). Ecological speciation may be especially prevalent on mountains, because spreading from the point of colonisation up- or down-slope (or sometimes around the different aspects of the mountain) necessarily involves movement across a succession of ecological clines, some of which may be very steep (both ecologically and physically) (Goodman et al. 2018; Scherz et al. 2023). However, the isolation of any location also varies according to the environmental tolerance and dispersal capacity of the lineage in focus, including its ability to use present dispersal vectors such as streams or wind (Flantua et al. 2020). Dispersal limitation is characterised by individuals being unable to reach environmentally suitable areas due to both spatial distance and barrier distance (i.e., distance to physical barriers or habitat dissimilarities such as temperature differences) or failure to adapt to less suitable niches (Eiserhardt et al. 2013).

Madagascar has several mountains, massifs, and mountain ranges formed by tectonic activity and volcanism (de Wit 2003), and given its large, ecologically highly variable area, is referred to as a 'micro-continent' (de Wit 2003; Vences et al. 2009; Glaw et al. 2022). It is also a biodiversity hotspot, with most of its endemic species being concentrated on and around its mountains (Ganzhorn et al. 2001; Wilmé et al. 2006; Wollenberg et al. 2008; Vences et al. 2009; Wesener et al. 2011; Brown et al. 2014, 2015, 2016; Wollenberg Valero 2015; Everson et al. 2020; Liu et al. 2024; Hazzi and Wood 2025). A promising study system for understanding mountain community assemblage and the potential role of ecological speciation can be found within the Madagascar-endemic, microhylid frog subfamily Cophylinae Cope, 1889: The genus *Stumpffia* Boettger, 1881 currently contains 44 recognized nominal species (Frost 2024) that range three-fold in body size, from some of the smallest frogs in the world, such as *S. contumelia* Rakotoarison et al., 2017 (8.0–8.9 mm snout–vent length [SVL]), to the much larger *S. staffordi* Köhler et al., 2010 (27.0–27.9 mm SVL) (Rakotoarison et al. 2017). As far as known, they are terrestrial frogs with ntidicolous tadpoles that are endotrophic, developing either in foam or jelly nests or in water-filled cavities, away from water bodies (Rakotoarison et al. 2017; Scherz et al. 2022). This gives them restricted vagility, especially in lineages that are miniaturised, and consequently *Stumpffia* species are often microendemic to single Malagasy mountains (Wollenberg et al. 2008; Rakotoarison et al. 2017).

Wollenberg et al. (2008) discussed the correlation between endemism and species richness in cophylines, indicating strong spatial niche conservatism and the crucial role of mountainous habitats for speciation. So far, the

Stumpffia assemblage of the Marojejy mountain massif in the northeast is the only one that has been studied in detail: Rakotoarison et al. (2019b) found intraspecific genetic differences between *Stumpffia sorata* Rakotoarison et al., 2017 and *Stumpffia tridactyla* Guibé, 1975 individuals collected at different elevations on the Marojejy massif, giving evidence that gene flow is impeded between different elevational populations. Both taxa occur over wide elevational ranges (Rakotoarison et al. 2019b). They also found species living in syntopy to differ from each other by their advertisement calls and calling activity time. At the species level the authors demonstrated that not a single species-pair has diverged *in situ* on Marojejy. This result might be explained by the comparatively high connectivity of Marojejy, directly connected at >1000 m a.s.l. with a larger mountain chain stretching across northern Madagascar.

Here, we present a study on the *Stumpffia* assemblage of another mountain in northern Madagascar: Montagne d'Ambre. This isolated, extinct volcano is situated at the northern tip of Madagascar, with its peak at 12.596°S, 049.152°E, with an elevation ranging from ~200 m a.s.l. to 1475 m a.s.l. (Gautier et al. 2018). It is covered by the Parc National de Montagne d'Ambre, a 30,689 ha protected area founded in 1958 (Goodman et al. 2018), and is characterised by a comparatively harsh transition zone between the humid rain forest of eastern Madagascar and the dry forests in western Madagascar (Hending et al. 2020). After Vences et al. (2012) proposed Montagne d'Ambre as an ideal model system to study anuran adaptive speciation, Scherz et al. (2023) demonstrated herpetofaunal community turnover and both morphological and genetic divergence linked to elevational zonation. At Montagne d'Ambre, six species of *Stumpffia* have been reported so far (Rakotoarison et al. 2017, 2022; Scherz et al. 2023): *Stumpffia angeluci* Rakotoarison et al., 2017, *S. huwei* Rakotoarison et al., 2017, *S. maledicta* Rakotoarison et al., 2017, *S. madagascariensis* Mocquard, 1895, *S. bishopi* Rakotoarison et al., 2022 and *S. megsoni* Köhler et al., 2010 (Rakotoarison et al. 2019b erroneously stated *Stumpffia achillei* Rakotoarison et al., 2017 to occur on Montagne d'Ambre—*S. angeluci* was meant). Building on this previous knowledge, we examined the diversity of *Stumpffia* occurring on Montagne d'Ambre based on morphometrics, phylogenetics, and bioacoustic data analysis and examine the potential biogeographic scenarios (i.e., *in situ* speciation vs. dispersal) to gain more understanding of the drivers of intra- and interspecific *Stumpffia* diversity on Montagne d'Ambre. For *in situ* diversified lineages, we predict a common phylogenetic origin and emerging reproductive isolation via segregation in quantitative bioacoustics traits, whilst conserving the general call structure (Köhler et al. 2017); opposed to that, we expect Montagne d'Ambre species that independently colonized the mountain to have distinct phylogenetic origins and to also differ in their call structure. Overall, we predict little morphometric differentiation in the *Stumpffia* species assembly, even along elevational clines, due to their reportedly conserved morphology with few exceptions (Rakotoarison et al. 2017).

Material and methods

Data acquisition

The majority of the data analysed here was collected on an expedition to Montagne d'Ambre carried out from November 2017 to January 2018 by Mark D. Scherz, Andolalao Rakotoarison, Safidy M. Rasolonjatovo, Jary H. Razafindraibe, Ricky T. Rakotonindrina, Onja Randraimalala, and Angeluc Razafimanantsoa; other results from this expedition have been reported elsewhere (Rasolonjatovo et al. 2020, 2022; Rakotoarison et al. 2022; Scherz et al. 2023). The expedition collected numerous *Stumpffia* specimens and tissue samples from across the mountain, including material from the herpetologically unexplored west slope of the mountain. Other samples included here were collected over numerous previous visits to the mountain over the past 25 years by various researchers.

Specimens were captured on surveys consisting of opportunistic and targeted searching by day and night (with the aid of hand-held and head torches), often guided by the calling activity of male specimens. Collected specimens were photographed in life, and voucher specimens were anaesthetised and subsequently euthanised using tricaine mesylate solution (MS222). A tissue sample of each individual was taken from limbs (either a muscle sample or, in small individuals, a whole part of the limb) and stored in 99% ethanol for molecular analysis. Voucher specimens were subsequently fixed in 90% ethanol, before permanent conservation in 70% ethanol. Field number labels were tied to specimens (or, in the case of diminutive individuals, affixed to Eppendorf tubes into which the frogs were placed). Field numbers used herein include **ACZCV** Angelica Crottini, **DRV** David R. Vieites, **FAZC** Franco Andreone, **FGMV** Frank Glaw and Miguel Vences, **FGZC** Frank Glaw, **MSZC** and **MSTIS** Mark D. Scherz, **RAX** Christopher J. Raxworthy, **RJS** Jasmin E. Randrianirina, and **ZCMV** and **MV** Miguel Vences. Specimens were deposited at the **ZSM** Zoologische Staatssammlung München, Munich, Germany, **UADBA** collections of the Mention Zoologie et Biodiversité Animale, Université d'Antananarivo, Antananarivo, Madagascar, and the **NHMD/ZMUC** Natural History Museum Denmark, Copenhagen, Denmark.

Sampling site

Montagne d'Ambre mostly consists of basalt, basanite, ankaratrite, covered by acidic Haplic Acrisols, Haplic Ferrasols and Haplic Cambisols (Goodman et al. 2018). It is entirely surrounded by sandstone, marl and shaley limestone (Donné et al. 2021). Despite plant growth limitation by high levels of aluminium and iron in the soil, the area is mostly covered by moist, evergreen forest with a canopy height of 20 to 25 m, whilst forests closer to the summit display a canopy usually below five metres (Goodman et al. 2018). Additionally, there is rather dry

vegetation (i.e., dry, deciduous forests) in a series of craters west of Lac Maudit, and along the west slope, largely due to porous underlying volcanic rock (Goodman et al. 2018). Montagne d'Ambre also contains several lakes, e.g., Lac Maudit and Grand Lac, which constitute noteworthy study sites for anuran ecology (Rasolontatovo et al. 2022). The local climate is dominated by the North-Malagasy subhumid climate, receiving annual average rainfall levels of about 1424 mm (in the years 1981–2017), the vast majority of which occurs between November and April as well as temperatures between 12.3°C (cold season: June–August) and 30.4°C, although temperatures decrease at the upper elevations (Goodman et al. 2018). Also, vegetation and the local climate (and thus, the fieldwork) are influenced by the regular occurrence of cyclones (Goodman et al. 2018; Rasolontatovo et al. 2020, 2022). Fieldwork in 2017–2018 was carried out along an elevational transect, with a satellite camp established on the West Slope (see Scherz et al. 2023 for further details). However, sampling gaps remain especially at the south slopes, the far east slopes, and the lowest elevations of the north slope.

DNA extraction, amplification, and sequencing

We obtained DNA sequences from the 3' and 5' fragments of the mitochondrial rRNA gene 16S and the nuclear-encoded Recombination Activation Gene (Rag1) of 45 specimens assigned to six nominal species in the course of this study. For this purpose, genomic DNA was extracted from muscle tissue or digits stored in 99% ethanol using either the standard salt extraction protocol by Bruford et al. (1992), or an SPRI Bead DNA Extraction Protocol (Phyletica Lab 2024) using Proteinase K (20 mg/ml) for digestion. Amplification via standard polymerase chain reaction (PCR) was performed according to protocols of Belluardo et al. (2022), using primers and PCR conditions as stated in Table S1 to a final volume of 25 µl per sample. PCR products were then purified by centrifugation through Sephadex G-50 Superfine (Cytiva, 17-0041-01) incubated in HPLC-H₂O (Merck, 1.15333.2500) in MultiScreen-HV plates (Millipore, 0.45 µm, MAHVN4510) according to the manufacturer's instructions, for five minutes at 910 × g. A volume of 5 µl of the resulting elute was added to each 2 µl 5× green GoTaq buffer (Promega GmbH), 0.5 µl Big Dye Terminator (v.3.1, ThermoFisher Scientific) 0.5 µl primer and 5.5 µl HPLC-H₂O (Merck, 1.15333.2500) to a total volume of 10 µl. Subsequently, 5 µl of this sequencing reaction was added to 5 µl HiDi Formamide (ThermoFisher Scientific, 4311320) on the Sanger sequencer (3500 Genetic Analyzer, ThermoFisher Scientific). The resulting forward and reverse sequence chromatograms were checked by eye and combined into a single contig for each sample and each marker. Sequences with low confidence due to deficient chromatogram quality were discarded. A further 117 sequences of the 3' 16S fragments were generated using the Illumina amplicon approach (Vences et al. 2016). Published 16S and

Rag1 sequences were downloaded from GenBank and included in the matrix in order to complete our sampling of *Stumpffia*, and we also incorporated a number of previously unpublished 16S and Rag1 sequences generated in the labs of A. Crottini and MV over the last fifteen years. We uploaded all novel sequences to GenBank (accession numbers: PX527161–PX527194 and PX600750–PX600957; Table S2).

Molecular phylogenetics

We produced four alignments with MAFFT online (Katoh et al. 2019) from newly generated and available sequences. All alignments were quality checked by eye with subsequent manual adjustments before testing for the optimal model for molecular evolution with the software jModelTest 2 version 2.1.10 (Darriba et al. 2012). GTR+I+G was determined as the optimal model for each individual alignment. *Anilany helenae* (Vallan, 2000) served as outgroup, since *Anilany* is phylogenetically sister to the genus *Stumpffia* (Scherz et al. 2016; Tu et al. 2018).

- Alignment A (length = 684 nt), consisting of 3' 16S sequences only, for a total of 315 *Stumpffia* specimens as well as a sequence from *Anilany helenae*.
- Alignment B (length = 680 nt), consisting of 5' 16S sequences only, for a total of 348 *Stumpffia* specimens as well as a sequence from *Anilany helenae*.
- Alignment C (length = 1238 nt), consisting of manually concatenated 3' and 5' 16S sequences, for a total of 59 *Stumpffia* specimens, aligned against a full 16S sequence from *Anilany helenae* (GenBank accession number MZ751042.1).
- Alignment D (length = 531 nt), consisting of Rag1 sequences only, for a total of 239 *Stumpffia* specimens as well as a sequence from *Anilany helenae*. Note that there were no sequences available for the Montagne d'Ambre endemic species *S. bishopi*.

For all four alignments, maximum likelihood trees were calculated using the software raxmlGUI version 2.0.7 (Edler et al. 2021), setting 'Analysis' to 'ML + rapid bootstrap' and 'Reps.' to 1000. For Alignment C, an additional Bayesian tree was calculated using MrBayes version 3.2.7 (Ronquist et al. 2012) using Markov chain Monte Carlo algorithm (MCMC), four chains, two runs and 2,000,000 generations. Trees for Alignments A, B, and C were displayed in FigTree version 1.4.4 (Rambaut 2018). Within the genus *Stumpffia*, four major clades are evident sensu Rakotoarison et al. (2017), clades A–D, which help to inform biogeographic analyses of the genus. All species of *Stumpffia* were included in our analyses, but only members of the A clade (sensu Rakotoarison et al. 2017) are depicted in figures for space reasons, as the other clades do not occur on Montagne d'Ambre. Non-focal clades are also collapsed in our figures. Full trees are

given in the supplementary material (Figs S1, S2). Full mean pairwise uncorrected p-distances were calculated based on the Alignment A, B, and C using the TaxI2 tool in iTaxoTools version 0.1 (Vences et al. 2021b).

A reduced version of Alignment D (length = 323 bp), containing no missing data and only including individuals of Clade A sensu Rakotoarison et al. (2017), was used to visualize the relationship among alleles (haplotypes) of *Rag1* using a network approach in the program Hapsolutely (Vences et al. 2024). Haplotypes were inferred using the PHASE algorithm (Stephens et al. 2001), using a phase (-p) and allele (-q) threshold of 0.5 with 1000 MCMC iterations. Based on the phased sequences, a network was constructed under the Median-Joining algorithm (Bandelt et al. 1999) and edited in Adobe Illustrator v29.4 (Adobe Inc., San Jose, CA, USA). The input files for Hapsolutely, along with the datasets for other analyses, are available from a dataset uploaded at the Zenodo repository at <https://doi.org/10.5281/zenodo.16385861>.

Bioacoustics

We analysed advertisement calls of various *Stumpffia* specimens from Montagne d'Ambre recorded over the last 20 years. Call series of different lengths were recorded from *Stumpffia angeluci* (MSZC 0531), *Stumpffia bishopi* (MSZC 0730), *Stumpffia huwei* (MSZC 0405, MSZC 0660, ZCMV 13618, ZCMV 13619, MSZC 0744, two series of MSZC 0769), *Stumpffia madagascariensis* (MSZC 0707, ZCMV 12185), *Stumpffia maledicta* (MSZC 0666, MSZC 0724, ZCMV 13504), *Stumpffia mamitika* (MSZC 0793), and *Stumpffia megsoni* (MSZC 0545, MSZC 0764, MSZC 0765, MSZC 0768, MSZC 0777). Calls from other locations were recorded for *S. angeluci* (ZCMV 13608, Joffreville) and *S. mamitika* (ZCMV 13616, Ankarana; one not-collected specimen, Andapa). Temperature data was unavailable for many recordings and is, thus, rarely given here. Calls are deposited in the Zenodo repository at <https://doi.org/10.5281/zenodo.16385861>. Note that recordings from ZCMV specimens were made with a damaged field recorder, which however mostly affected their amplitude profiles only, and does not appear to have had detrimental effects on the fidelity of call frequencies.

Recordings were resampled at 22.05 kilohertz (**kHz**) and analysed in Audacity (Audacity Team 2014). Call duration was calculated by identifying the start and end of calls in waveform view. Duration of the inter-call interval (from the end of one call to the start of the next) was calculated subsequently. Dominant frequencies were obtained from plotted spectra of single calls. Results were displayed as ‘minimum – maximum (mean \pm standard deviation)’ in milliseconds (**ms**) or respectively in Hertz (**Hz**), according to Rakotoarison et al. (2017). We define a call of *Stumpffia* herein as a single, high-pitched tonal note (Rakotoarison et al. 2017) and use the terminology for call descriptions by Köhler et al. (2017), using the call-centered terminological scheme. Inter-call intervals varied quite substantially even within a call series, raising

the question of whether well-motivated calling specimens were recorded and thus, do not seem to be a suitable character for species identification in this assemblage. Plots of call duration vs. dominant frequency were created using the ggplot2 package (Wickham 2016) in R (R Core Team 2024) with RStudio (RStudio Team 2019).

Morphometrics

Basic morphometric measurements were taken on a total of 64 specimens from seven nominal species and one potential candidate species: *Stumpffia angeluci* (N = 13), *Stumpffia bishopi* (N = 3), *Stumpffia huwei* (N = 14), *Stumpffia madagascariensis* (N = 4), *Stumpffia maledicta* (N = 12), *Stumpffia mamitika* (N = 9), *Stumpffia megsoni* (N = 6), and *Stumpffia* sp. aff. *angeluci* (N = 3). All specimens were collected on Montagne d'Ambre, except for three individuals of *S. mamitika* (ZSM 3237/2012, ZSM 0307/2004, ZSM 0228/2016) and five specimens of *S. angeluci* (ZSM 300–303/2004, ZSM 1671/2008).

Morphological measurements followed Rakotoarison et al. (2017), and were the following: **SVL** snout–vent length, **HW** maximum head width, **HL** head length, **TD** horizontal tympanum diameter, **ED** horizontal eye diameter, **END** eye–nostril distance, **NSD** nostril–snout distance, **NND** nostril–nostril distance, **FORL** forelimb length, **HAL** hand length, **HIL** hindlimb length, measured straightened, **FOTL** foot length including tarsus, **FOL** foot length without tarsus, and **TIBL** tibia length. Additionally, **UAL** upper arm length, **LAL** lower arm length, **THIL** thigh length, and **TARL** tarsus length were taken. We did not examine the relative position of the tibiotarsal articulation position when stretched forward along the body to avoid damaging specimens. A measurement scheme is given in Figure 1. All measurements were performed using digital callipers (Mitutoyo Corp., CD-15DAX, accuracy \pm 0.02 mm; Mitutoyo Corp., CD-15CP, accuracy \pm 0.03 mm; Hogetex, Digital Caliper, 6M05.3.42, accuracy \pm 0.03 mm). Measurements were subsequently compared to previous measurements from Rakotoarison et al. (2017, 2022), but to avoid inconsistencies due to measurer effect, only newly obtained measurements obtained by a single measurer were retained for analyses.

Morphometrics were used to perform a principal component analysis (**PCA**) in RStudio (RStudio Team 2019) with R (R Core Team 2024), using the ggplot2 (Wickham 2016) and tidyverse (Wickham et al. 2019) packages. To avoid losing specimens due to missing data, three hind limb measurements were imputed for four specimens of *Stumpffia huwei* from the west slope (MSTIS 00930, 00931, 00964, and 00967) by linear regression against SVL. One specimen, ZSM 0228/2016 (ZCMV 13616), was omitted due to a missing measurement of FORL. PCA was performed for the following traits: $\log_{10}(\text{SVL})$, HW, HL, TD, ED, END, NSD, NND, FORL, HAL, HIL, FOTL, FOL, TIBL, UAL, LAL, THIL, TARL. Values other than SVL were corrected for relative size by taking their residuals from a linear model against SVL.

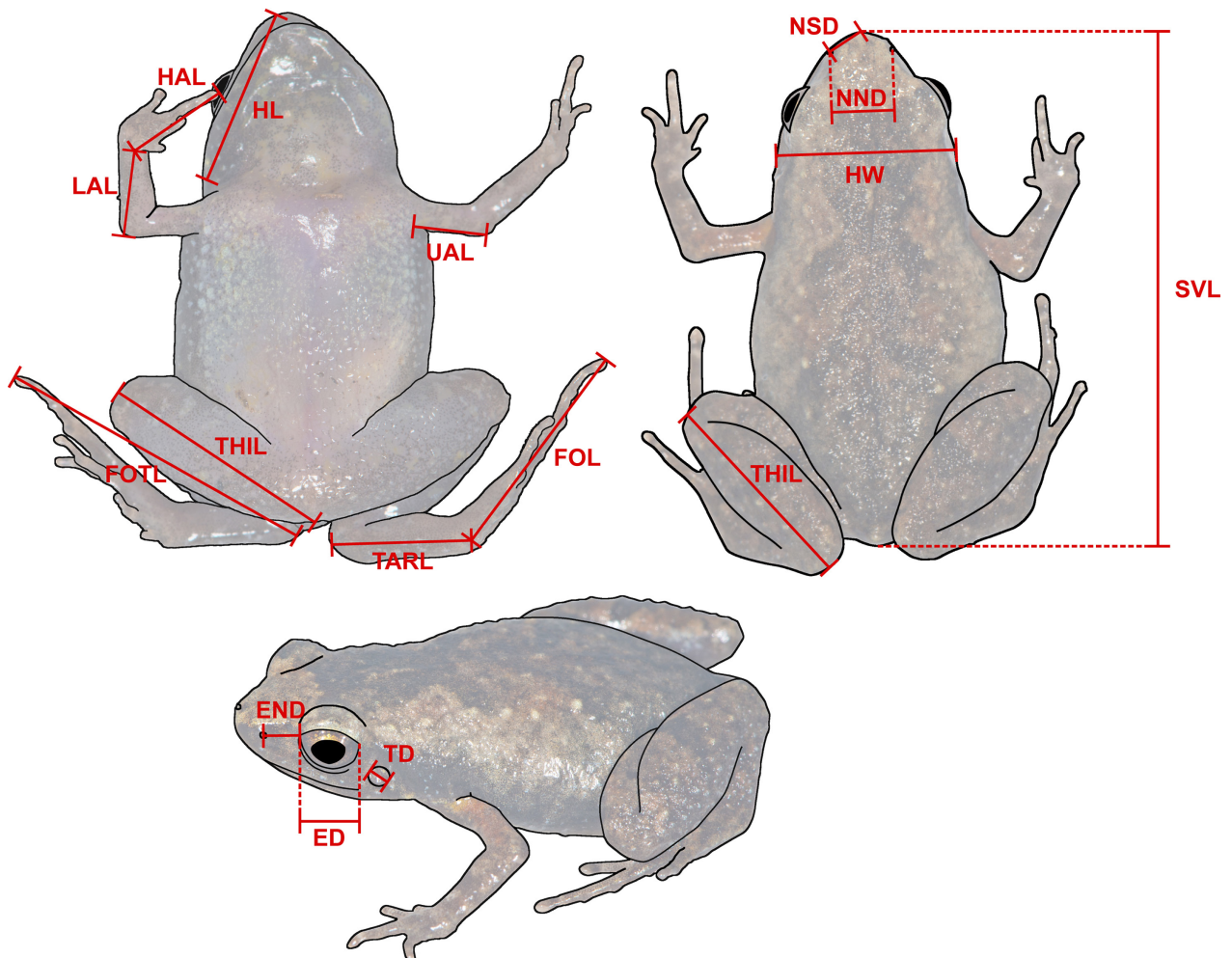


Figure 1. Measurement scheme based on Rakotoarison et al. (2017) supplemented by UAL, LAL, THIL, and TARL, displayed in *Stumpffia mamitika* (ZSM 116/2018, field number MSZC 0793). Note, that FOTL would be measured with foot and tarsus stretched in a straight line. FORL and HIL are not displayed herein.

Results

Identity and variability of *Stumpffia* on Montagne d'Ambre

A total of 91 *Stumpffia* specimens and tissue samples were collected on Montagne d'Ambre (Fig. 2) between October 2017 and January 2018, including nine call vouchers (i.e., males observed and recorded calling). Sequences of the mitochondrial 16S rRNA markers we analysed, successfully assigned all sequenced individuals to species level (Figs 3, S1–S4), and confirmed the presence of the following species: *Stumpffia angeluci* (seven specimens), *S. bishopi* (three specimens), *S. huwei* (22 specimens), *S. madagascariensis* (14 specimens), *S. maledicta* (30 specimens), *S. mamitika* (one specimen), *S. megsoni* (13 specimens), *S. sp. aff. angeluci* (three specimens) (Figs 3, 4, S4). *Stumpffia* sp. aff. *angeluci* represents a previously unknown lineage, and *Stumpffia mamitika* is here reported from Montagne d'Ambre for the first time.

We recovered remarkably high infraspecific variation in *Stumpffia huwei*, notably between the populations from

the west and north slopes; they differ by uncorrected pairwise distances (p-distances) of 1.68–2.09% in the 5' 16S fragment of Alignment B (Table S3). However, two specimens from near the Gîte d'Étape (ZCMV 3996 collected in 2009 and MSZC 0643) on the north slope also differed by 1.17–2.17% in the 5' 16S fragment from other individuals from the same locality (Table S3). Nevertheless, uncorrected p-distances from the 3' 16S fragment (Alignment A) that is more frequently used for species delimitation in Malagasy anurans (Vieites et al. 2009) are only high between the west and north slope specimens (up to 1.65%) but do not differ strongly between specimens of the same location. These west slope specimens are clearly differentiated from other *S. huwei* in the phylogenetic trees calculated, with strong support (Fig. 3; Table S4).

Concurrently with their genetic differentiation, west slope specimens of *S. huwei* show differences in bio-acoustics and morphometrics compared to those from the north slope (Fig. 5; Table S5). Dominant call frequency shows zero overlap in the measured parameters between west slope specimens and other specimens of *S. huwei* (5120–5515 Hz from west slope specimens MSZC 0744 and MSZC 0769 vs. 4615–5057 Hz from north slope

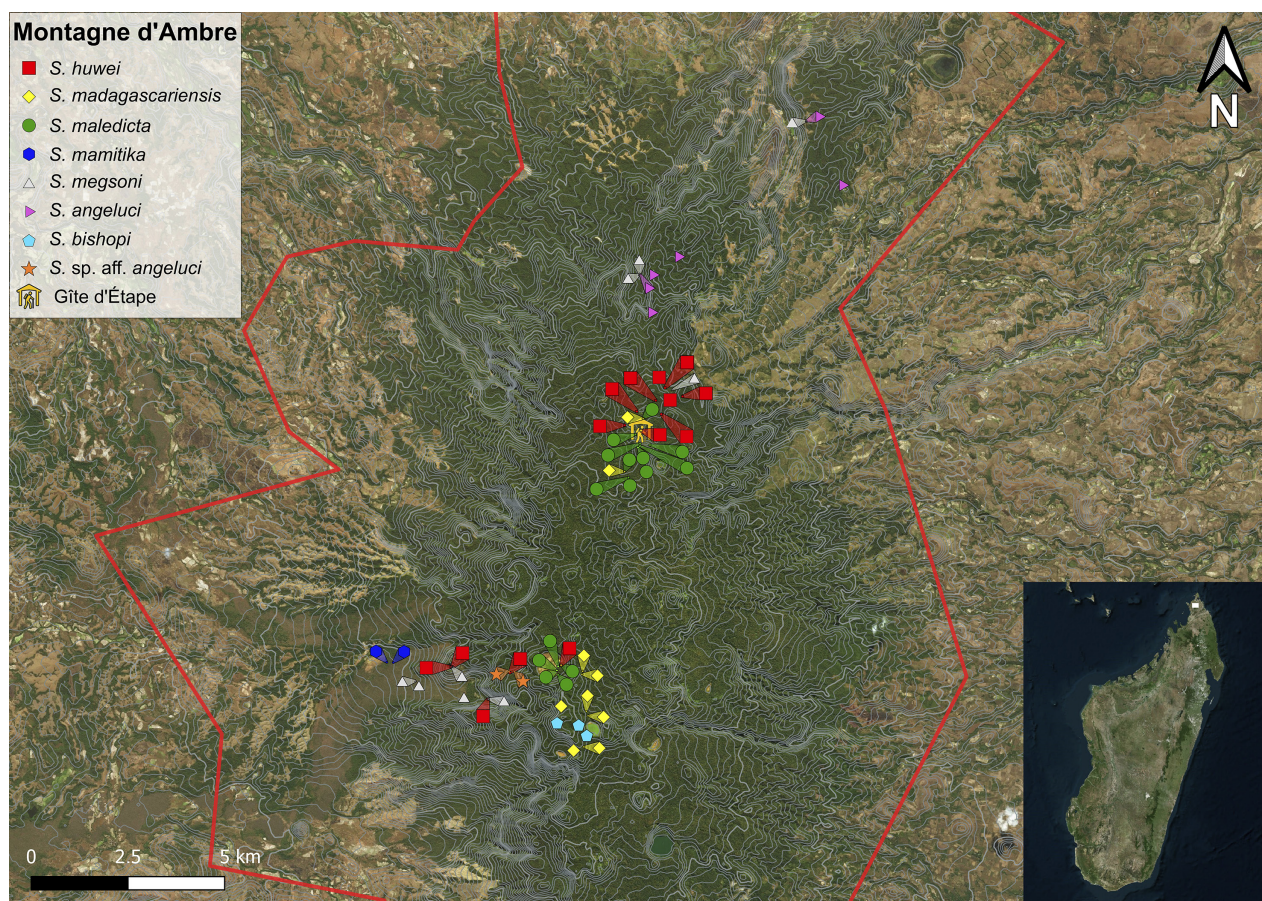


Figure 2. Map of Montagne d'Ambre in Northern Madagascar, displaying collection sites from the expedition as well as the guest house, Gîte d'Étape. The red line marks the border of Parc National de Montagne d'Ambre. Thin white contour lines represent 20 m elevation steps, thick white contours 200 m. Inset map shows the position in Madagascar, indicated by a white rectangle. Satellite imagery from Bing Maps, 2022.

specimens; Table 1), despite being highly similar in body size on average (Fig. 5). However, call duration and inter-call intervals are not substantially different, partly due to high standard deviations within call series of single individuals. Morphometrically, west slope specimens and other members of *S. huwei* differ in only few traits (Table S5): West slope specimens have on average longer upper arms (UAL) without overlapping values with other specimens of *S. huwei* and, thus, longer forelimbs (FORL), with or without scaling to body size (SVL). Although there is substantial overlap in PCs 1 and 2 of our morphometric PCA (Fig. 6), they have almost no overlap in PC3, which is weighted most strongly by ED, THIL, UAL, and FORL (Fig. S5).

The specimen of *S. mamilika* found on Montagne d'Ambre (ZSM 116/2018, field number MSZC 0793) also differs in bioacoustics from conspecifics from other locations (Fig. 7), without overlap in dominant frequency (5369–5781 Hz in ZSM 116/2018 vs. 4417–4626 Hz in other calling males of *S. mamilika*; Table 1). The spectrograms reveal that ZSM 116/2018 displays not just a harmonic of the other specimens' dominant frequencies (which seems to be the case for the *S. madagascariensis* specimens; Fig. 8) but emits calls with a different fundamental frequency (Figs 7, 8). As in *S. huwei*, call duration and inter-call intervals are not substantially different,

partly due to high standard deviations within call series of single individuals. Morphometrically, ZSM 116/2018 differs only very slightly in tympanum diameter (TD/SVL) and eye–nostril distance (END/SVL) from other *S. mamilika* but displays otherwise values within the range for the species in the remaining traits (Table S5). It does, however, differ strongly from conspecifics in the 5' 16S sequences by unpaired p-distances of 0.51–2.95; it was not sequenced for the 3' 16S fragment (Table S3).

Phylogenetic analysis revealed a highly divergent lineage containing MSZC 0436, MSZC 0710, and ZCMV 13048, which we now tentatively label as *Stumpffia* sp. aff. *angeluci* (Figs 3, S4). All three specimens are from the vicinity of Lac Maudit. They are closest to *Stumpffia angeluci*, with p-distances of 3.00–3.19% in the 3' 16S sequences (Table S4) and 3.05–3.86% to them in the 5' 16S sequences (Table S3). In the short Illumina-sequenced 3' 16S fragment, they exhibit lower p-distances towards *Stumpffia maledicta* (1.50% to all), but the longer 5' fragment contains more informative sites. They overlap in morphospace with *S. angeluci* (Figs 6, S5), but a more detailed morphological analysis may reveal further differences; these specimens warrant recognition as an unconfirmed candidate species (Vieites et al. 2009).

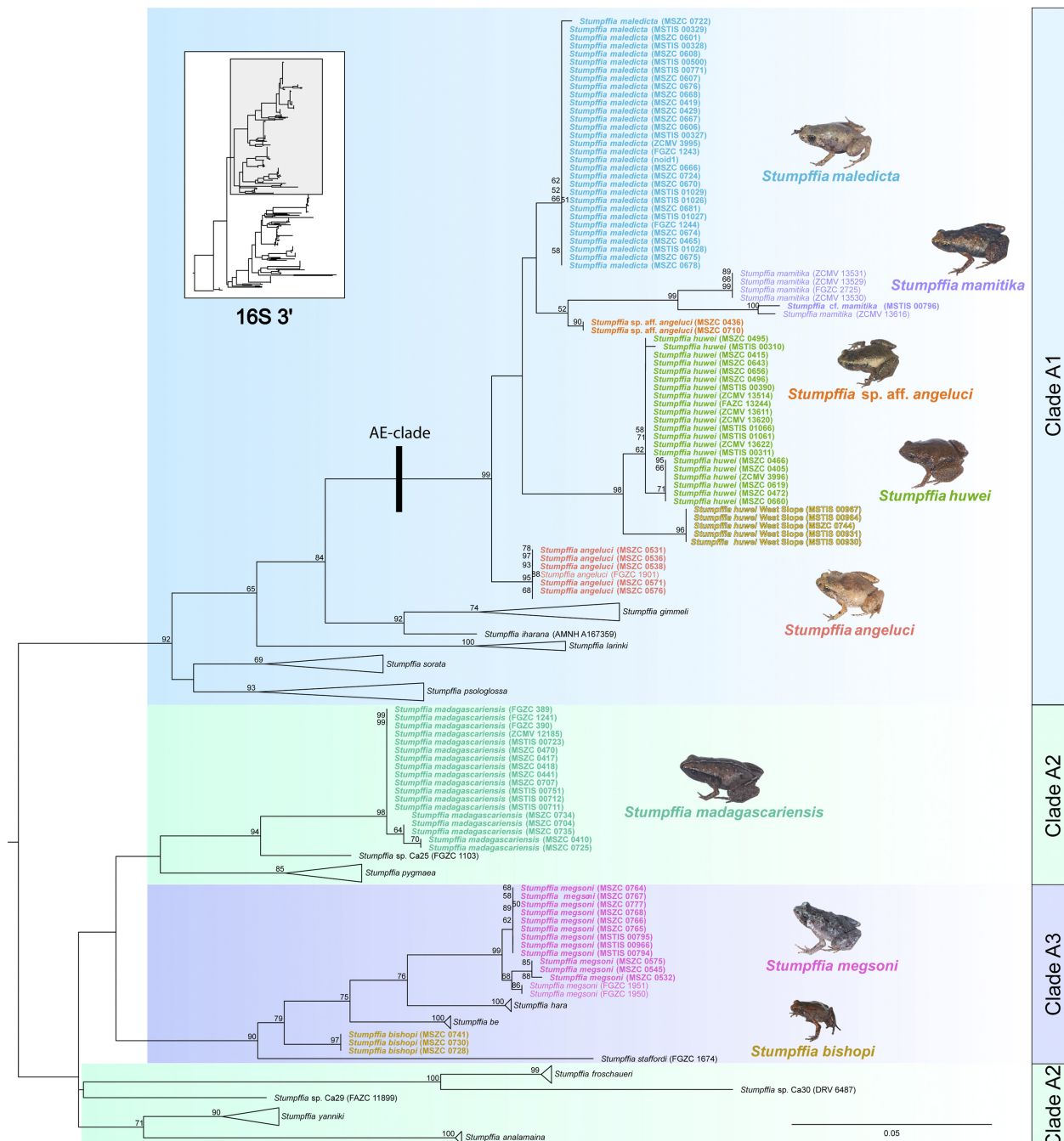


Fig. 3. Maximum likelihood phylogenies of *Stumpffia* based on Alignment A (16S 3'). Only members of Clade A according to Rakotoarison et al. (2017) are shown; their position in the overall *Stumpffia* phylogeny is indicated by a grey rectangle. Specimens from Montagne d'Ambre are bolded. “AE-clade” refers to the Ambre-endemic clade. Node labels are given as bootstrap values, not displayed when below 50. For the full phylogeny see Figure S2.

Assemblage of *Stumpffia* on Montagne d'Ambre

In the phylogenetic tree calculated based on Alignment C (3'+5' 16S; Figs 9, S3), some of the Montagne d'Ambre species together form a monophyletic group, containing *S. maledicta*, *S. huwei*, *S. mamitika*, *S. angeluci*, and *S. sp. aff. angeluci*. We refer to this clade herein as the ‘Ambre-endemic clade’ (AE-clade); *S. maledicta*, *S. huwei*, and *S. sp. aff. angeluci* are, according to current knowledge, microendemic to Montagne d'Ambre, whereas *S. mamitika* is also found in other parts of northern Mad-

agascar as much as 240 km away (Vohemar, Ankarana, Andapa) and *S. angeluci* has been recorded on Montagne des Français, 35 km away (Rakotoarison et al. 2017). This latter species also occurs at the lowest elevations on Montagne d'Ambre (Fig. 4H). In addition to this clade, the phylogenetically distant *Stumpffia madagascariensis* and *S. bishopi* are also microendemic to Montagne d'Ambre. The diminutive *Stumpffia madagascariensis* (9.7–11.9 mm SVL; Rakotoarison et al. 2017; note, fig. 26a, b in that paper shows a specimen incorrectly assigned to this species that is substantially larger; it is probably *S. angeluci*) is sister to the candidate species *S. sp. Ca25* from

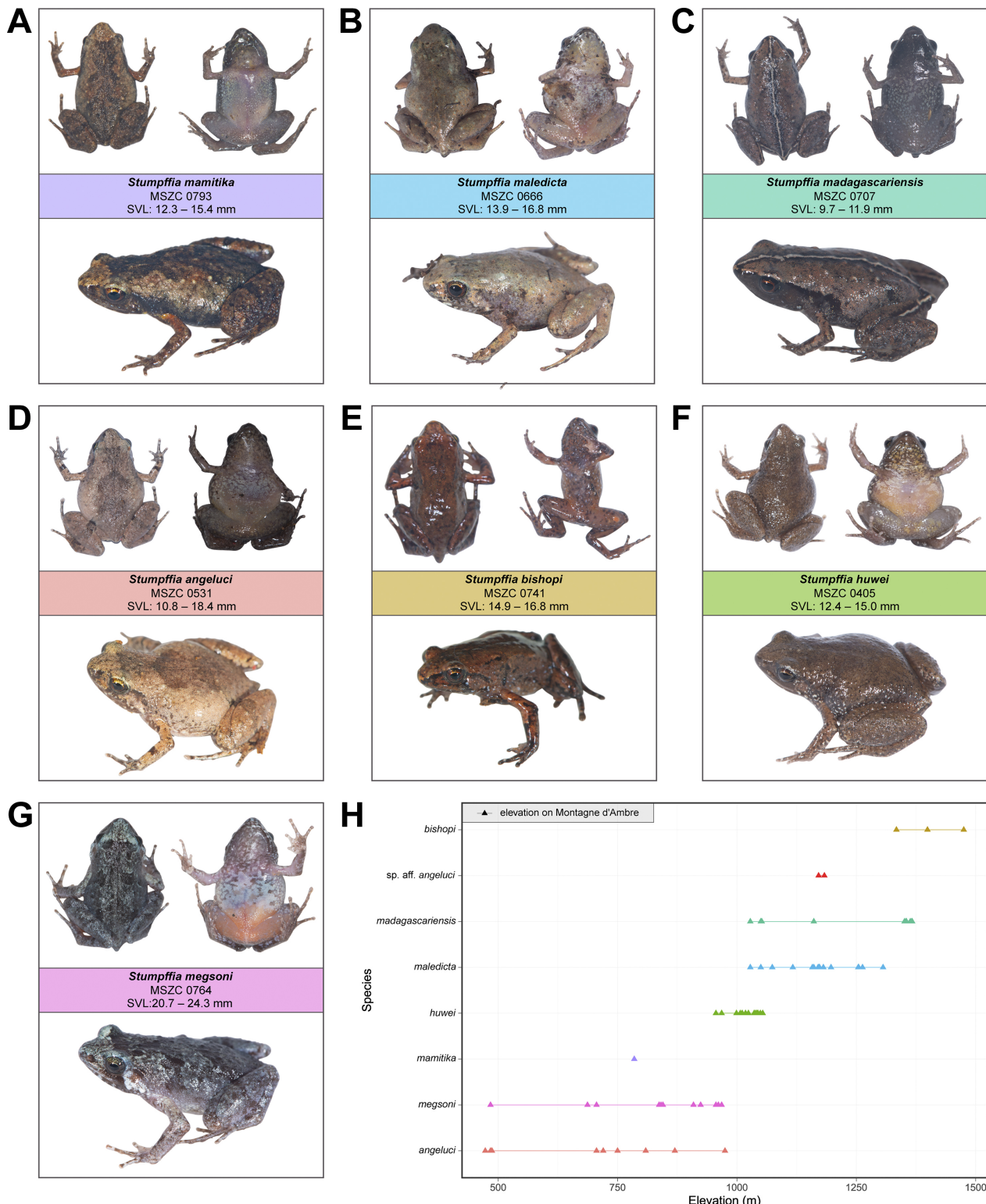


Figure 4. The *Stumpffia* assemblage of Montagne d'Ambre, Madagascar. **A–G** Photographs of dorsal, ventral, and dorsolateral view of *Stumpffia* species occurring on Montagne d'Ambre. Snout–vent lengths (SVL) are given as range of minimum – maximum values recorded for each species. For origin of SVL data see ‘Material and methods’ section. **H** Elevational distribution of *Stumpffia* species collected on Montagne d'Ambre. Each triangle represents a single collected specimen/tissue sample. Elevations are given in meters above sea level (m a.s.l.). Species are sorted by lowest minimal elevation (bottom) to highest minimal elevation (top).

Montagne des Français, about which very little is known. *Stumpffia bishopi* and *S. megsoni*, the latter also occurring in dry forests further north, form a clade with *S. be Köhler et al., 2010*, *S. hara* Köhler et al., 2010, and *S. staffordi* Köhler et al., 2010 (Figs 3, 9, S4). Whether *S. bishopi* or

S. staffordi is the sister taxon of the remaining lineages in this clade differs between the 16S 3' tree (Fig. 3) and both the 16S 5' tree (Figs S1, S4) and the concatenated tree based on Alignment C (Figs 9, S3). However, since *S. bishopi* is a lineage diverging from a very basal node

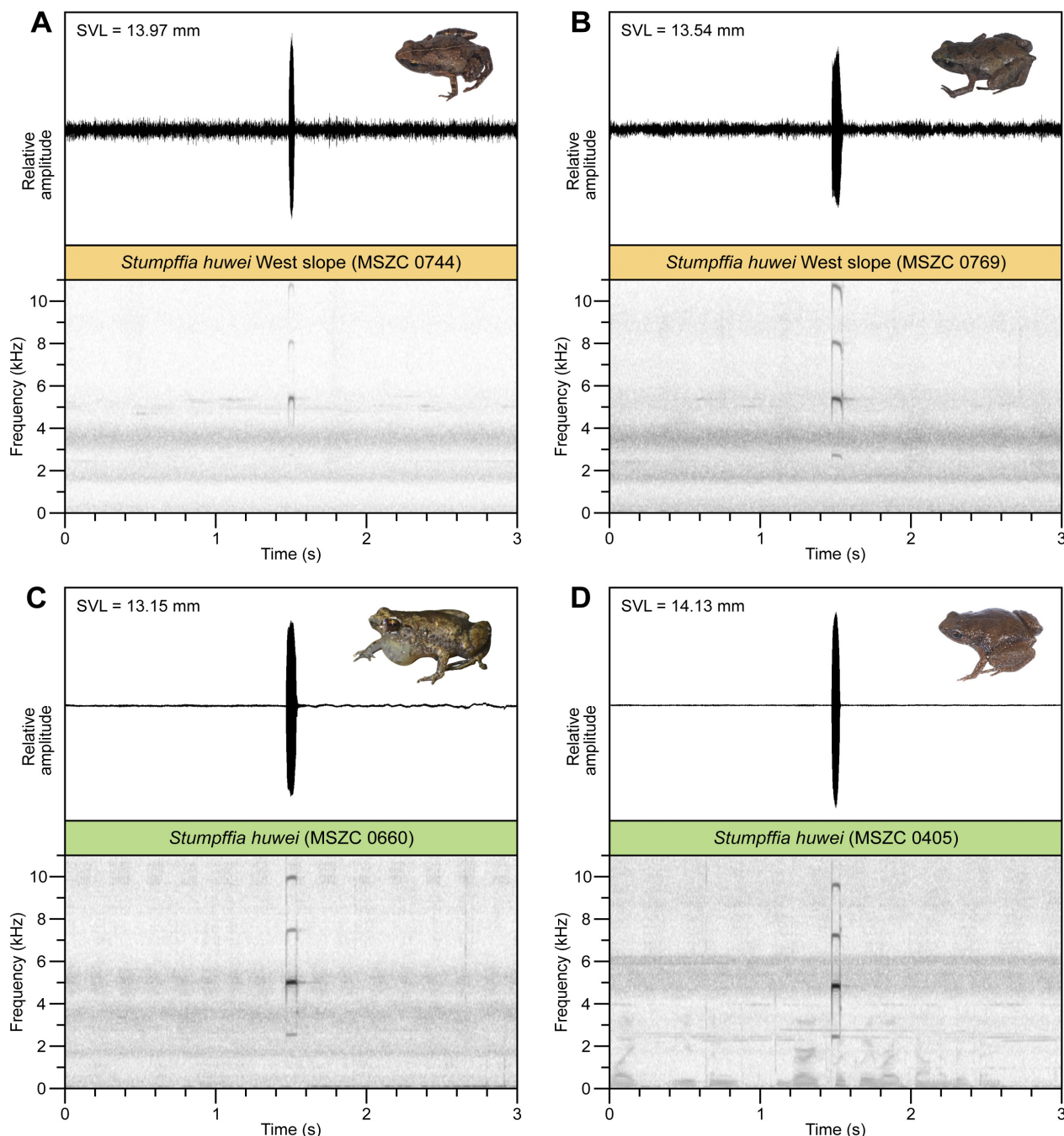


Figure 5. Bioacoustic data from *Stumpffia huwei*, shown as waveforms (above) and spectrograms (below) from one call each over an interval of 3 s. Spectrograms are visualised using Hanning windows with 256 bands resolution and 75% window width. Calls were recorded from **A** MSZC 0769 and **B** MSZC 0744 from the west slope and **C** MSZC 0660 and **D** MSZC 0405 from other sites of Montagne d'Ambre. Body size is given as SVL in the upper left corner of each waveform plot.

whilst *S. megsoni* is a later-diverging lineage, they most likely have different origins on the mountain.

Montagne d'Ambre *Stumpffia* species show multiple cases of haplotype sharing in the nuclear *Rag1* marker (Fig. 10): *Stumpffia huwei* and *S. angeluci*; *S. maledicta* and *S. angeluci*; *S. huwei* and *S. maledicta*; *S. mamilika* and *S. sorata*; and *S. mamilika* and *S. gimmeli*. *Stumpffia gimmeli* and *S. sorata* are not found on Montagne d'Ambre, but both species are rather widespread and contain significant intraspecific genetic diversity (Rakotoarison et al. 2017, 2019b). *Stumpffia megsoni* and *S. madagascariensis* are each separated from their genetically closest

species by multiple mutation steps and show no signs of haplotype sharing.

Morphological differentiation of Montagne d'Ambre *Stumpffia*

Montagne d'Ambre specimens contain medium to large-sized *Stumpffia*, ranging in body size (SVL) from 9.7 mm in *S. madagascariensis* to 24.3 mm in *S. megsoni* (Figs 4, 6). *Stumpffia angeluci* seems to be larger on average on Montagne d'Ambre compared to the other

Table 1. Bioacoustic analysis for species of *Stumpffia* found on Montagne d’Ambre. Specimens were recorded on Montagne d’Ambre if not indicated otherwise. One specimen of *S. mimitika* was not caught and thus has no collection/field number. Values are given as ‘minimum – maximum (mean \pm standard deviation, N = number of examined calls or call intervals)’. Few temperatures were taken due to equipment failure.

Field number	Species	Call duration	Inter-call interval duration	Dominant Frequency
ZCMV 13608	<i>Stumpffia angeluci</i> (Joffreville)	178–186 ms (183.5 \pm 2.7 ms, N = 7)	3271–3449 ms (3365 \pm 61.9 ms, N = 6)	4519–4551 Hz (4532.7 \pm 10.9 Hz, N = 7)
MSZC 0531	<i>Stumpffia angeluci</i>	159–183 ms (171.2 \pm 5.1 ms, N = 34)	3005–6330 ms (3523.5 \pm 620.5 ms, N = 31)	4084–4314 Hz (4193.1 \pm 74.6 Hz, N = 34)
MSZC 0730	<i>Stumpffia bishopi</i>	111–120 ms (116.2 \pm 2.4 ms, N = 22)	4404–6394 ms (5316.5 \pm 622.7 ms, N = 14)	3876–4243 Hz (4007.4 \pm 100 Hz, N = 22)
MSZC 0405	<i>Stumpffia huwei</i>	57.9–69.9 ms (64.9 \pm 2.8 ms, N = 36)	2754–6284 ms (3358 \pm 842.2 ms, N = 34)	4615–4855 Hz (4761.4 \pm 66.5 Hz, N = 36)
MSZC 0660	<i>Stumpffia huwei</i> , 19.0°C	70.9–88 ms (78.3 \pm 3.6 ms; N = 61)	2148–4413 ms (2493.2 \pm 341.2 ms, N = 60)	4731–5035 Hz (4866.7 \pm 86.8 Hz, N = 61)
MSZC 0744	<i>Stumpffia huwei</i>	34–55.9 ms (47.9 \pm 8 ms, N = 14)	3437–6406 ms (3928.4 \pm 902.4 ms, N = 11)	5120–5468 Hz (5372.5 \pm 98.5 Hz, N = 14)
MSZC 0769	<i>Stumpffia huwei</i>	60–76 ms (70 \pm 3.3 ms, N = 38)	2242–4789.9 ms (2668.5 \pm 430.6 ms, N = 37)	5175–5515 Hz (5329.1 \pm 121.2 Hz, N = 38)
MSZC 0769	<i>Stumpffia huwei</i>	43–57.9 ms (53 \pm 6.8 ms, N = 4)	2797–2941 ms (2869.6 \pm 72 ms, N = 3)	5313–5339 Hz (5326.2 \pm 12.6 Hz, N = 4)
ZCMV 13618	<i>Stumpffia huwei</i>	68–69.9 ms (68.9 \pm 1.4 ms, N = 2)	2762 ms (N = 1)	5012–5013 Hz (5012.5 \pm 0.7 Hz, N = 2)
ZCMV 13619	<i>Stumpffia huwei</i>	65.9–68 ms (66.9 \pm 1.4 ms, N = 2)	2750 ms (N = 1)	5057–5057 Hz (5057 \pm 0 Hz, N = 2)
MSZC 0707	<i>Stumpffia madagascariensis</i> , 18.4°C	184–205 ms (199.5 \pm 6.6 ms, N = 9)	7229–13281 ms (10447.1 \pm 2460.6 ms, N = 7)	5715–6195 Hz (5900.6 \pm 152.7 Hz, N = 9)
ZCMV 12185	<i>Stumpffia madagascariensis</i>	205–207 ms (205.7 \pm 0.9 ms, N = 4)	3933–4105 ms (4008.6 \pm 87.8 ms, N = 3)	3979–4015 Hz (3994.2 \pm 16.5 Hz, N = 4)
MSZC 0666	<i>Stumpffia maledicta</i> , 17.3°C	117–129 ms (123.3 \pm 3.1 ms, N = 38)	3139–8369 ms (4597 \pm 1463.6 ms, N = 37)	4221–4486 Hz (4404.1 \pm 60.3 Hz, N = 38)
MSZC 0724	<i>Stumpffia maledicta</i> , 18.5°C	97.9–122 ms (113 \pm 4.9 ms, N = 51)	2514–8994 ms (3834.4 \pm 1144.5 ms, N = 50)	4028–4295 Hz (4139.3 \pm 52.6 Hz, N = 51)
ZCMV 13504	<i>Stumpffia maledicta</i>	117–123.9 ms (119.7 \pm 3 ms, N = 4)	5146–6611 ms (5907.3 \pm 734.2 ms, N = 3)	4823–4844 Hz (4829.2 \pm 10 Hz, N = 4)
Not collected	<i>Stumpffia mimitika</i> (Andapa)	85.9–91.9 ms (88.8 \pm 1.8 ms, N = 8)	1362–4883 ms (2119.8 \pm 1239.9 ms, N = 7)	4428–4532 Hz (4494.3 \pm 35 Hz, N = 8)
MSZC 0793	<i>Stumpffia mimitika</i> , 18–19°C	69–88.9 ms (82 \pm 5.5 ms, N = 57)	951.9–3743 ms (2326.8 \pm 446.5 ms, N = 50)	5369–5781 Hz (5518.9 \pm 142.9 Hz, N = 57)
ZCMV 13616	<i>Stumpffia mimitika</i> (Ankarana)	68.9–79.9 ms (72.7 \pm 4.9 ms, N = 4)	1348–1893 ms (1579 \pm 281.8 ms, N = 3)	4580–4626 Hz (4600.2 \pm 22.8 Hz, N = 4)
MSZC 0545	<i>Stumpffia megsoni</i> , 21.7°C	96–114 ms (102.8 \pm 3.4 ms, N = 50)	938–1161 ms (1020.5 \pm 49.5 ms, N = 49)	3301–3434 Hz (3372.2 \pm 28.2 Hz, N = 50)
MSZC 0764	<i>Stumpffia megsoni</i>	134–147.9 ms (141.4 \pm 3.1 ms, N = 50)	1728–5221 ms (2225.1 \pm 635.1 ms, N = 48)	3098–3323 Hz (3267.2 \pm 36.1 Hz, N = 50)
MSZC 0765	<i>Stumpffia megsoni</i>	109–118 ms (112.9 \pm 2.1 ms, N = 30)	1455–5712 ms (2199.5 \pm 910.1 ms, N = 28)	3348–3523 Hz (3436.4 \pm 55 Hz, N = 30)
MSZC 0768	<i>Stumpffia megsoni</i>	111–127 ms (122.8 \pm 3.7 ms, N = 15)	1583–2093 ms (1778 \pm 125.9 ms, N = 14)	3115–3251 Hz (3209.3 \pm 39.5 Hz, N = 15)
MSZC 0777	<i>Stumpffia megsoni</i>	107–123.9 ms (116.1 \pm 4.2 ms, N = 15)	1654–2945 ms (1906.5 \pm 386.6 ms, N = 12)	3185–3376 Hz (3290.4 \pm 48.6 Hz, N = 15)

specimens of the same species that were collected on Montagne des Français (Table S6). Morphometrically, all species are rather similar, and only few species lack overlap in a plot of PC1 and PC2 of our size-corrected PCA (Fig. 6): *Stumpffia madagascariensis* is the most distinct, overlapping in morphospace only with *S. huwei*. *Stumpffia* sp. aff. *angeluci* is also moderately distinct, overlapping in morphospace only with *S. angeluci* and *S. maledicta*. Although *S. megsoni* is much larger than all other species, this is evidently not associated with shape changes beyond standard allometry, as it

overlaps in morphospace with most other taxa. Body size differs to only a limited extent among species, with *S. megsoni* being much larger, and *S. madagascariensis* much smaller, than all other species (Fig. 6). *Stumpffia angeluci* shows particularly great variation in body size, from 10.8 to 18.4 mm; we cannot discount that some of the smallest measured specimens may be juveniles or subadults. While qualitative characters were not measured in this study, it is noteworthy that slightly expanded finger discs are only known from *S. megsoni* (Köhler et al. 2010).

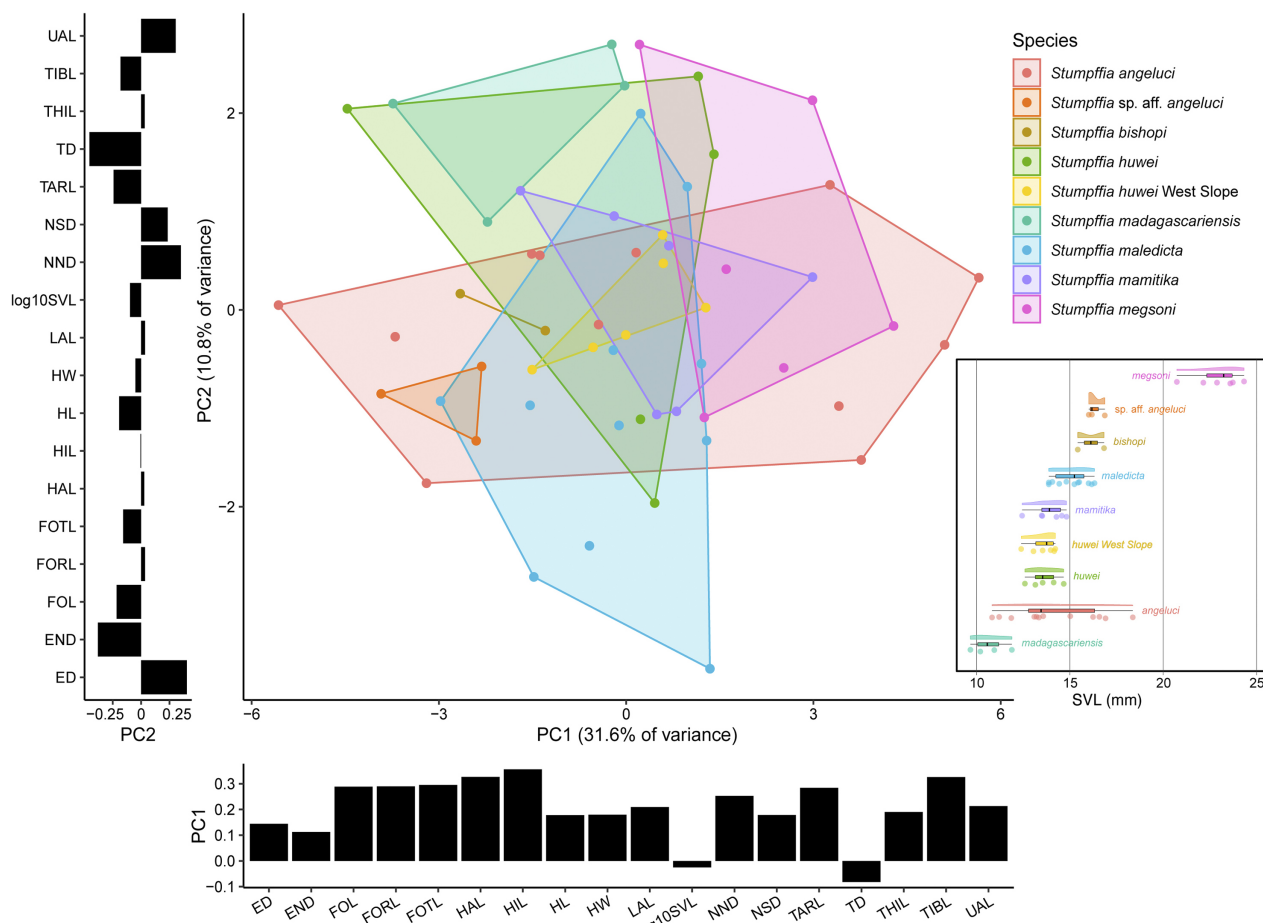


Figure 6. Principal component analysis (PCA) of size-corrected morphometric data and body size of *Stumpffia* that occur on Montagne d'Ambre (raw data in Table S5). Bar charts show weightings of measurements on respective principal components. Inset plot shows relative body size (snout–vent length) across the assemblage. Size-residuals of all measurements other than SVL were used.

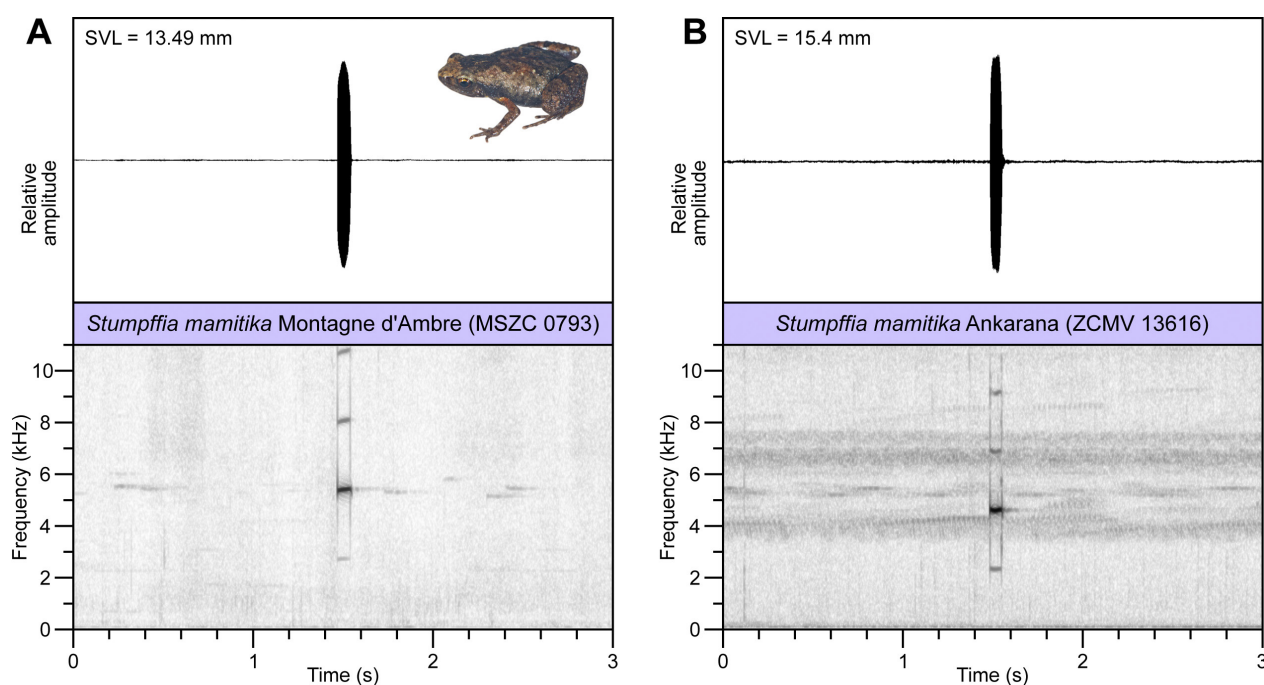


Figure 7. Bioacoustic data from *Stumpffia mamilika*, shown as waveforms (above) and spectrograms (below) from one call each over an interval of 3 s. Spectrograms are visualised using Hanning windows with 256 bands resolution and 75% window width. Calls were recorded from **A** MSZC 0793 from Montagne d'Ambre (individual shown in the inset) and **B** ZCMV 13616 from Ankarana (the type locality). Body size is given as SVL in the upper left corner of each waveform plot.

Bioacoustic differentiation of Montagne d'Ambre *Stumpffia*

We analysed calls of 23 individuals belonging to seven species (Table 1; only *S. sp. aff. angeluci* was not recorded calling), which consist of single short tonal notes resembling a high-pitched ‘beep’, and are repeated in a call series of variable duration. Intraspecific variation was moderate,

except in inter-call intervals, which varied substantially even intra-individually (i.e., within single call series). Dominant frequencies showed only little variation within a call series, but in some cases varied substantially within a species (Table 1), e.g., in *S. huwei* (4615–5515 Hz). Most extreme are the differences in dominant frequencies in the two analysed calls of *S. madagascariensis* (3994 Hz for ZCMV 12185 vs. 5901 Hz for MSZC 0707 on average;

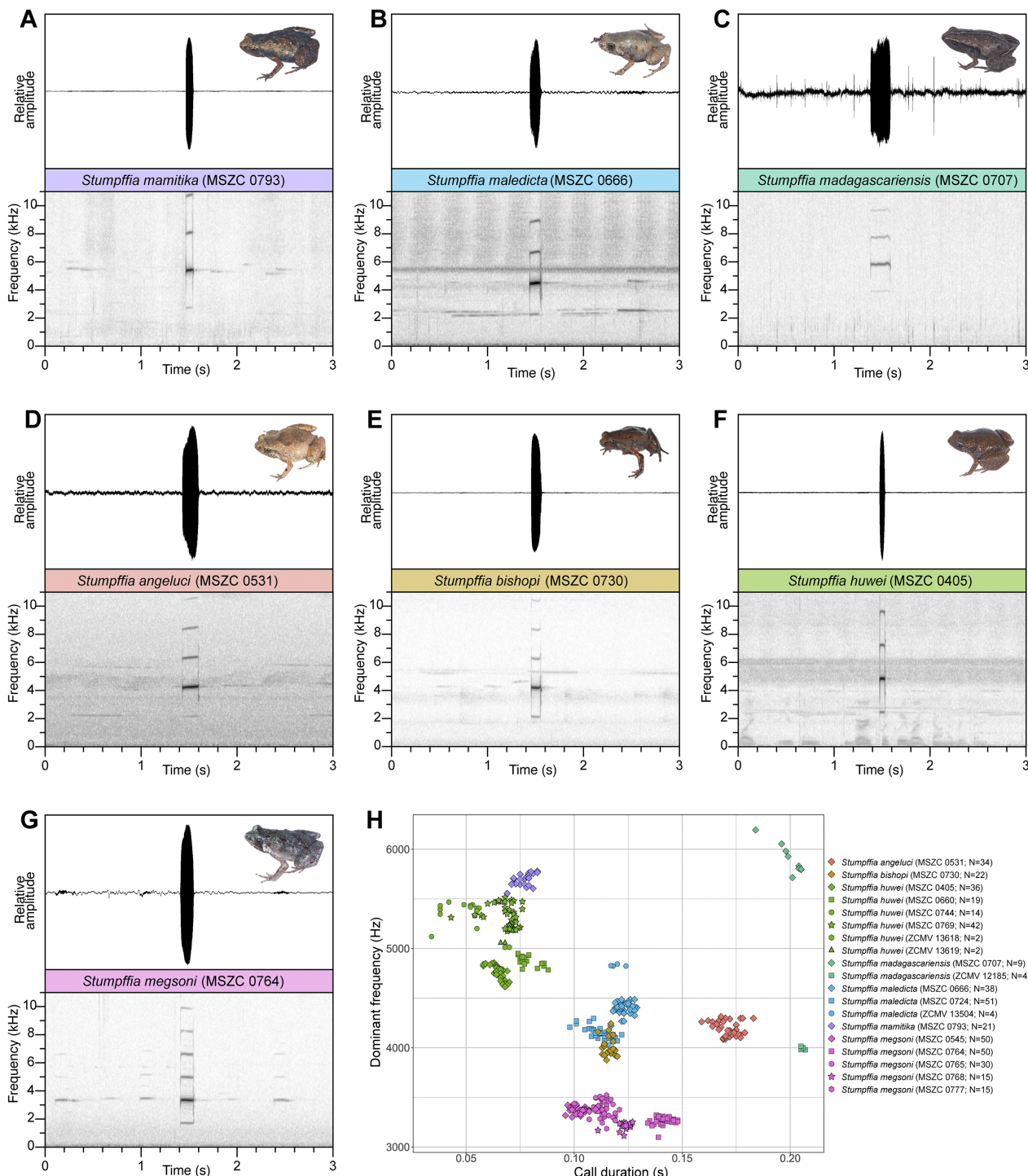


Figure 8. Bioacoustic data from *Stumpffia* calls A–G shown as waveforms (above) and spectrograms (below) of one call each with a time interval of 3 s. Spectrograms are visualised using Hanning windows with 256 bands resolution and 75% window width. All calls were recorded on Montagne d'Ambre. Dorsolateral photographs of the males assigned to each call are displayed, except for *S. bishopi* (photograph shows MSZC 0741). **H** Dominant frequencies plotted against call durations from Montagne d'Ambre *Stumpffia* specimens.

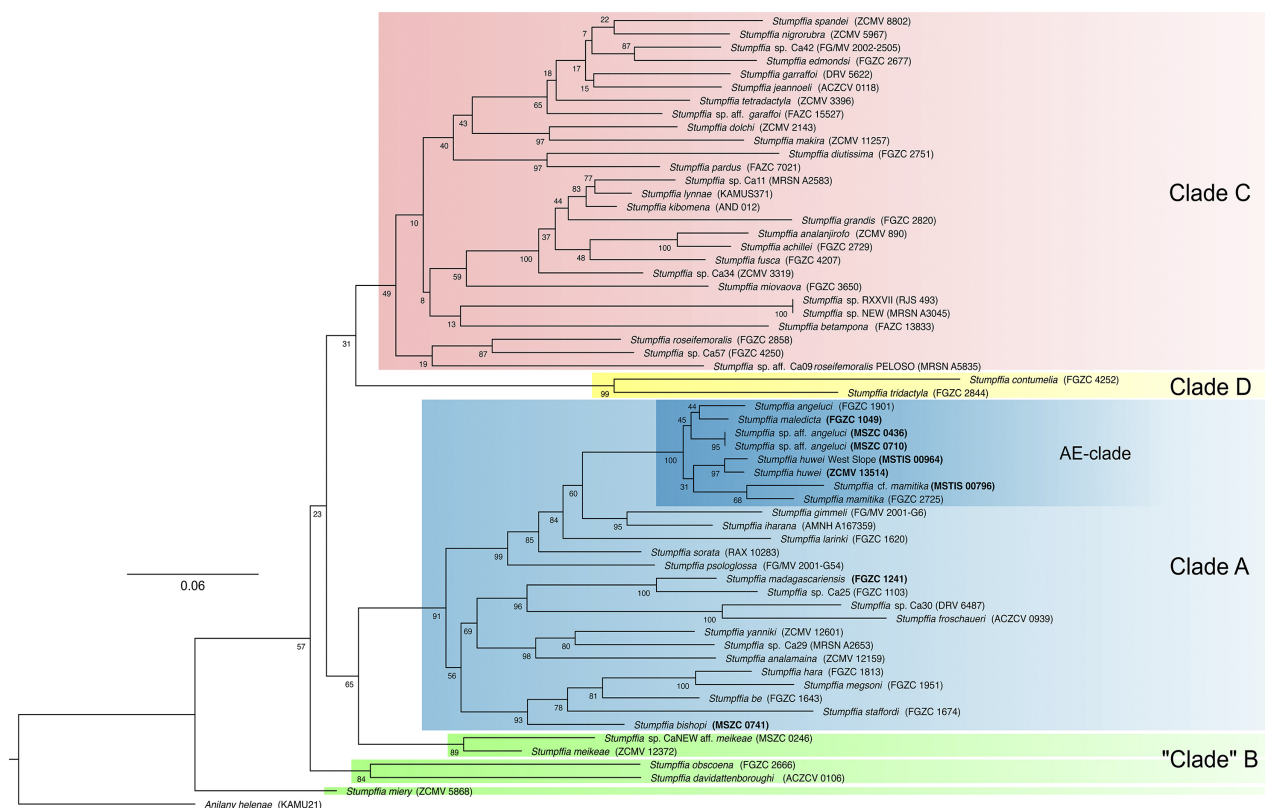


Figure 9. Maximum likelihood phylogeny of *Stumpffia* based on the concatenated Alignment C (3'+5' 16S). “AE-clade” refers to the Ambre-endemic clade. Node labels are given as bootstrap values. Bolded species and specimens indicate occurrence on Montagne d’Ambre.

Fig. 8H), but this appears to be due to the dominant frequency being on a different harmonic of calls with a shared fundamental frequency around 2000 Hz (harmonics of the call of MSZC 0707 can be seen in Fig. 8C), which might be linked to different recording distances (Köhler et al. 2017). Frequency modulation is either absent or little expressed in Montagne d’Ambre *Stumpffia* (Fig. 8A–G). No frequency modulation was found in *S. madagascariensis*, *S. bishopi*, and *S. huwei*; slight upward modulation was present in Montagne d’Ambre *S. mimitika* (absent in Ankarana specimen, Fig. 7), *S. maledicta*, and *S. angeluci*; slight downward (or no) modulation was detected in *S. megsoni*.

The community of *Stumpffia* on Montagne d’Ambre—comprising a mixture of a micro-endemically radiated species, micro-endemic species belonging to more widespread clades, and at least one more-widespread species—exhibits strong call differentiation among species (Fig. 8; Table 1), especially among species co-occurring at the same elevation. Different species occurring at the same elevation emit calls that differ drastically interspecifically (compare Fig. 4H to Fig. 8H). For example, *Stumpffia mimitika*, *S. megsoni*, and *S. angeluci* are all found (though not exclusively) at 785 m a.s.l. and emit calls with dominant frequencies of 4428–5781 Hz (*S. mimitika*), 3098–3523 Hz (*S. megsoni*) and 4084–4551 Hz (*S. angeluci*). The small overlap between *S. mimitika* and *S. angeluci* is actually due to inclusion of specimens of *S. mimitika* from Ankarana; the only specimen of *S. mimitika* recorded on Montagne d’Ambre (MSZC 0793) called

at dominant frequencies of 5369–5781 Hz, i.e., >800 Hz higher than the maximum dominant frequency recorded from *S. angeluci*. More importantly, call duration ranges of those three species also do not overlap, which are—in contrast to frequency—Independent of body size (Köhler et al. 2017).

Calls of Montagne d’Ambre *Stumpffia* are so distinct that we have been able to provide a dichotomous key to their identification (Appendix). Note that this key only applies to reasonably motivated individuals calling on Montagne d’Ambre and may else fail.

Discussion

Our results show that there are at least seven, and possibly eight, species of *Stumpffia* on Montagne d’Ambre, rather than the six that were previously known (Rakotoarison et al. 2017). Four of the seven species are microendemic to Montagne d’Ambre, according to current data available (*S. bishopi*, *S. madagascariensis*, *S. maledicta*, *S. huwei*), as well as the new unconfirmed candidate species, *Stumpffia* sp. aff. *angeluci* (MSZC 0436, MSZC 0710, ZCMV 13048). Additional specimens, ideally calling males, of this lineage should be collected to allow a comprehensive taxonomic assessment. Nonetheless, the emerging picture is one of remarkable diversity for a single mountain.

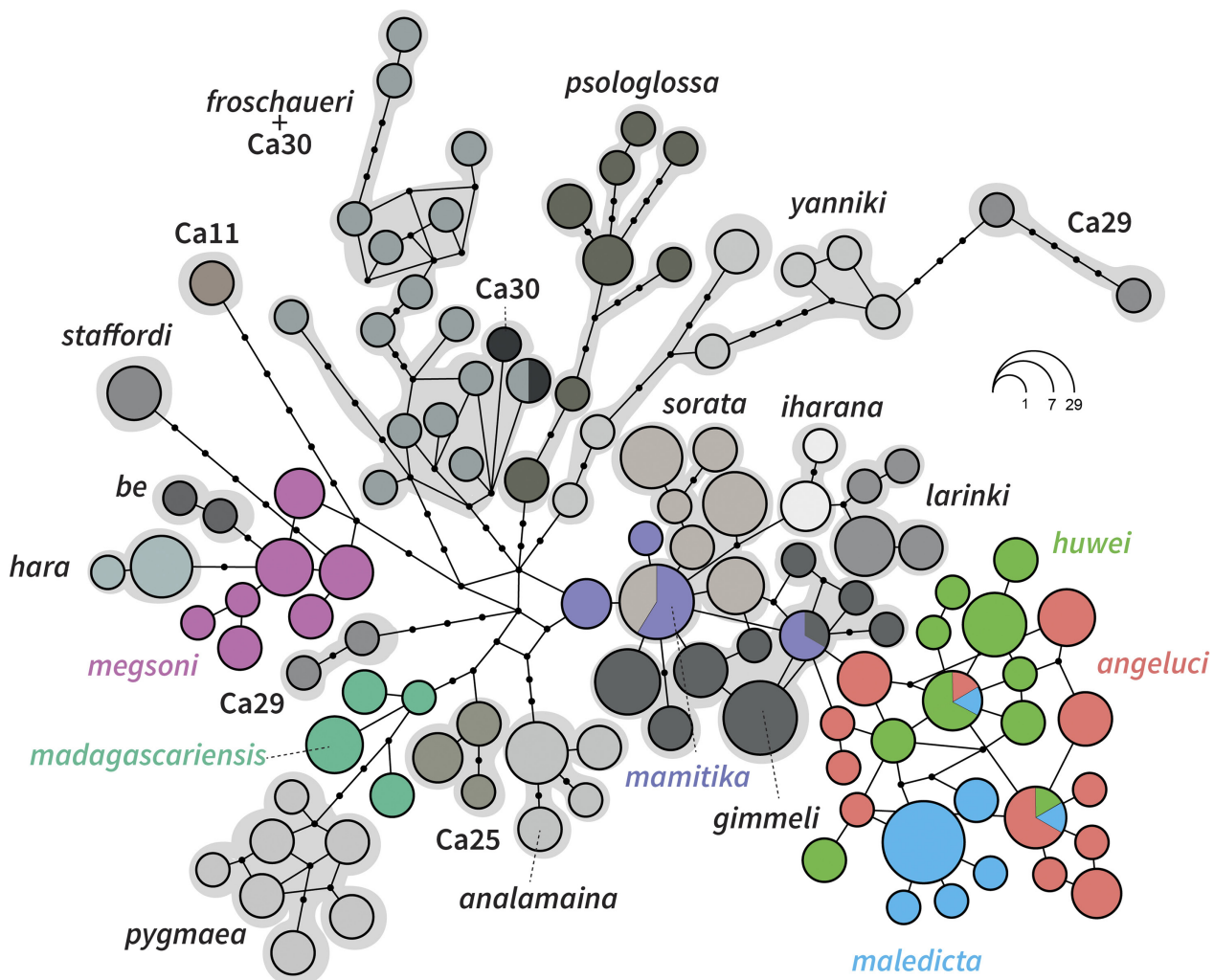


Figure 10. Rag1 ($n = 151$; length = 323 bp) haplotype network of Clade A sensu Rakotoarison et al. (2017). Circles represent haplotypes, with size proportional to allele frequency. Dots on the branches indicate the number of mutational steps between haplotypes. The Montagne d'Ambre-endemic *S. bishopi* has not been sequenced for this marker.

This assemblage exhibits conserved morphology. Except for outliers at the upper and lower extremes of body size in these frogs, our PCA highlights the lack of distinct morphometric differences among species (Figs 6, S5), though it does not account for differentiation in qualitative traits like slightly expanded finger discs in *S. megsoni* (Köhler et al. 2010). In contrast, however, there is strong biogeographical and bioacoustic segregation (Figs 4H, 8H). Several new elevational records resulted in an updated elevational distribution map of *Stumpffia* species occurring on Montagne d'Ambre (Figs 2, 4H). For *S. mamilika*, for example, verified elevational data have been recorded only at 121 m a.s.l. in Ankarana previously (Rakotoarison et al. 2017). The new data extends this range to a new maximum elevation of 785 m a.s.l., based on a genetically confirmed sample.

Bioacoustically, all species differ substantially in dominant frequency and/or call duration in their advertisement calls, except *S. bishopi* and *S. maledicta*. However, they do not overlap in their elevational distribution. Conversely, species occurring in spatial proximity (e.g., *S. megsoni* and *S. huwei*; Fig. 2) show intense segregation in their calls (Fig. 8H). The call of *S. mamilika* on Montagne

d'Ambre is substantially higher in dominant frequency than low-elevation specimens from Ankarana, which may be a reflection of differing body sizes (Köhler et al. 2017), but could also be a result of local co-occurrence with *S. angeluci*, which calls at a similar dominant frequency at this elevation (Figs 4H, 8H). Such differentiation could in principle trigger a cascading reinforcement and lead to evolution of reproductive barriers over time (Ortiz-Barrientos et al. 2009; Nosil 2012). The Montagne d'Ambre *Stumpffia* assemblage may be an excellent candidate for simple, experimental studies on sexual selection based on advertisement calls.

The species assemblage on any given mountain may be the result of several, independent colonization events or initial colonization and subsequent in situ diversification (Fig. 11). Montagne d'Ambre has a wealth of micro-endemic fauna (Goodman et al. 2018). Scherz et al. (2023) uncovered both intraspecific genetic and community-level differentiation of herpetofaunal species along the strong elevational ecotone on Montagne d'Ambre. They concluded that this may promote ecological speciation among a wide variety of organisms along a common gradient. The observed distribution and diversity of

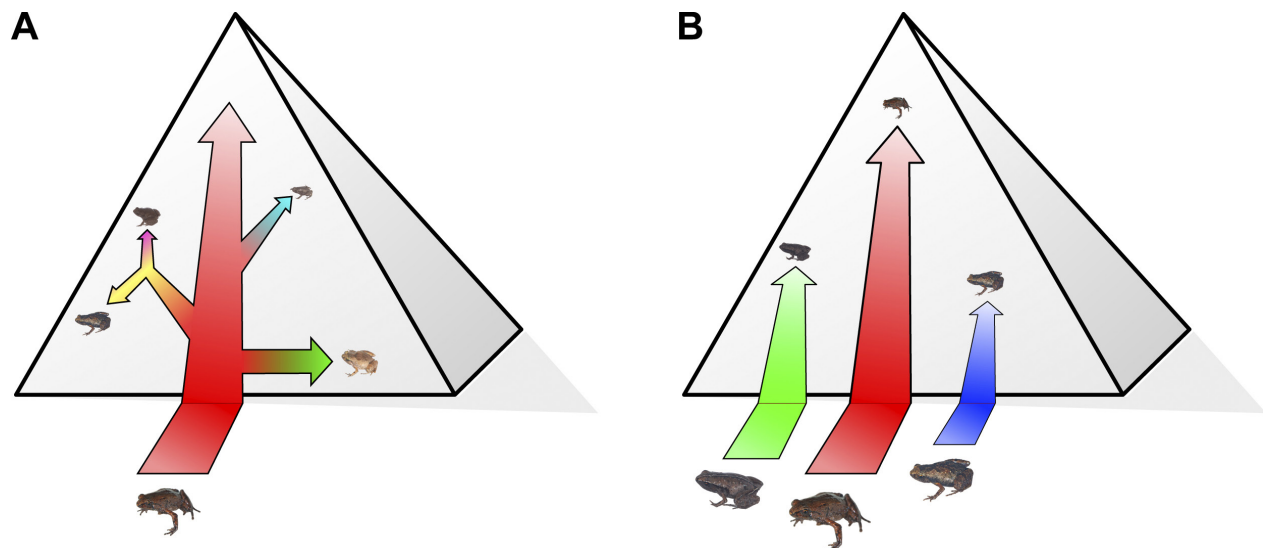


Figure 11. Modes of dispersal on isolated mountains in non-airborne animals. **A** Single colonisation event with subsequent in situ speciation and **B** multiple, independent colonisation events.

Stumpffia is consistent with this. *Stumpffia* have colonised Montagne d'Ambre at least four separate times (Figs 3, 9; multigene tree in Rakotoarison et al. 2017), and there is substantial turnover in species up the slope of the mountain (Fig. 4H). The AE-clade, consisting exclusively of species found on Montagne d'Ambre (Fig. 9), including the microendemic taxa *S. maledicta* and *S. huwei*, may have originated on the mountain. The close relatedness of the AE-clade is also highlighted by the high similarity in the call structure (Köhler et al. 2017) in Montagne d'Ambre *S. mamilika*, *S. maledicta*, and *S. angeluci*, i.e., a slightly upward frequency modulation. On the other hand, no frequency modulation was detected in *S. madagascariensis* and *S. bishopi*, and a downward frequency modulation was found in *S. megsoni*. However, the current phylogenetic resolution of our trees is insufficient to draw strong conclusions on the exact evolutionary origins of Montagne d'Ambre *Stumpffia*.

Moreover, we discovered substantial genetic variation within some lineages, e.g., *S. huwei*, which indicates (1) that our understanding of the genetic diversity of *Stumpffia* species on the mountain is far from complete, and (2) that there may be ongoing diversification across the mountain's heterogeneous habitats, which differ both by elevation and by aspect. Haplotype sharing in Rag1 among some species (Fig. 10) may reflect standing genetic variation or incomplete lineage sorting (ILS), especially for geographically distantly occurring species, but within Montagne d'Ambre it could also point toward the existence of ongoing gene flow. Population genetics approaches would be needed to clarify this.

Rakotoarison et al. (2019b) investigated the *Stumpffia* assemblage on the Marojejy massif in northern Madagascar in a comparable way to this study, enabling the comparison of these two assemblages and their respective origins. Both assemblages consist of circa seven species (Marojejy: *Stumpffia tridactyla*, *S. cf. sorata*, *S. grandis*, *S. sp. Ca11*, *S. roseifemoralis*, *S. diutissima*, *S. achillei*). No species are shared between the mountains,

although *S. mamilika* is found near the foot of Marojejy, at Andapa. We have here shown that *Stumpffia* have remarkable bioacoustics variability on Montagne d'Ambre; Rakotoarison et al. (2019b) did not include bioacoustics of Marojejy's *Stumpffia*, but we may predict that they will be similarly differentiated, and can anecdotally report that there is an additional factor, time of day at which species call, which seems to differ among co-occurring species at ca 1300 m a.s.l. at least (MDS, MV, AR, pers. obs.). Variability of calls within species on Marojejy will be particularly interesting to compare.

In contrast to Montagne d'Ambre *Stumpffia*, Rakotoarison et al. (2019b) found all *Stumpffia* species occurring on Marojejy to be phylogenetically distant from each other, and thus to have colonised the massif independently, without indication of potential in situ speciation—though some evidence for emerging intraspecific diversification in *S. tridactyla* was provided. This is remarkable, as Marojejy seems to be a more promising area for in situ speciation than Montagne d'Ambre: The Parc National de Marojejy covers a surface area of 55,885 ha (vs. 30,689 ha, Parc National de Montagne d'Ambre), a greater elevational range and steeper ecotone over 75–2132 m a.s.l. (vs. 200–1475 m a.s.l. on Montagne d'Ambre), and has a broader range of vegetation zones (e.g., montane scrub, sclerophyllous montane cloud forest, and bamboo forest; Goodman et al. 2018). It is geologically substantially older, and granitic as opposed to volcanic (Goodenough et al. 2010; Cucciniello et al. 2011). The biodiversity of birds, reptiles, and amphibians is estimated to be greater on Marojejy than on Montagne d'Ambre (Goodman et al. 2018). We might therefore expect a greater diversity of *Stumpffia*, and for at least some to have diversified in situ.

Setting is a key difference between these two areas. Whereas Montagne d'Ambre is practically isolated from any other rainforest, Marojejy is part of a larger complex of massifs and ridges that extends across northern Madagascar and south as the island's eastern mountain range,

potentially allowing the dispersal of nearby mountain species into this, hence, less isolated area. This opposition in connection may be the key factor behind the disparities in the origins of the respective communities of *Stumpffia* on the two mountains. However, it is important to emphasise that practically every visit to Marojejy in recent years has yielded new species of amphibians, and our picture of its community may still be far from complete. Moreover, no other sites have yet had their *Stumpffia* assemblages studied in comparable detail. The vast majority of mountainous areas in northern Madagascar remain herpetologically under- or unexplored.

Microendemism has been found to be strongly linked to mountainous habitats in Cophylinae (Wollenberg et al. 2008). Colonisation by non-flying animals of an isolated mountain usually starts at its lowest elevation (with rare exceptions, e.g., dispersal of smaller animals via strong cyclones) (Antonelli et al. 2018). It is expected that there will be more micro-endemism at higher elevation, and conversely, more widespread species to occur at lower elevations (Steinbauer et al. 2016). This pattern is evident in Montagne d'Ambre, with widespread species at lower elevation, and micro-endemics at higher elevations. Different elevational zones have differing climate, biodiversity, and vegetation types, and hence, up-slope displacement necessarily involves adaptation across a succession of ecological clines. *Stumpffia* at the highest elevations of Montagne d'Ambre (e.g., *S. bishopi*; Fig. 4H) may have arisen from lineages that adapted across each ecological zone of the mountain below their current maximum elevation over their evolutionary history. However, they could also have reached modern distribution without adaptation if they moved along with shifting microclimate due to major climate fluctuations. Species occurring over very broad elevational ranges may have greater environmental tolerance, increasing their ability for adaptation to different habitats.

The potentially *in situ* speciated, monophyletic AE-clade (Figs 3, 9) not only includes multiple microendemic lineages but also shows intense elevational zonation (Fig. 4H), indicating a link between elevation and speciation in mountainous *Stumpffia*. Future work should investigate the population genetics, extent of gene flow, thermal tolerance, and sexual selection of this diverse radiation, which may serve as an excellent model to understand the multifarious action of a shared ecotone on speciation in a taxon with low vagility.

Acknowledgements

We are grateful to the Malagasy authorities in the Ministère de l'Environnement et du Développement Durable and Madagascar National Parks for providing permissions. Fieldwork in Montagne d'Ambre was conducted under the permits 19117-MEEF/SG/DGF/DSAP/SCB.R dated 24 July 2017 and financed by the Deutsche Forschungsgemeinschaft (DFG) grant VE 247/13-1 to MV and MDS. Samples were exported under permit no. 032N-EA02/ MG18 dated 14 February 2018. We are grateful to Ella Z. Lattenkamp, Ricky T. Rakotonindrina, Onja Randriamalala, Safidy M. Rasoloniato, Jary H. Razafindraibe, Fano-

mezana M. Ratsoavina, Zafimahery Rakotomalala, and local guides for assistance in collecting data in the field. We thank Sebastian Steinfartz for support given to NJF in development and execution of this work. We further want to thank Michael Franzen for the provision of tissue samples, and Frank Glaw for valuable input regarding the planning of fieldwork. We thank Angelica Crottini for access to hitherto unpublished DNA sequences that we were able to incorporate in our alignments. We also thank Michael Hofreiter and Ralph Tiedemann for permission to use the laboratory facilities of the University of Potsdam and Katja Havenstein, Silke Abelt and Michaela Preick for their assistance in lab work. This work was funded by Deutsche Forschungsgemeinschaft grants VE 247/13-1 and SCHE 2181/1-1 (part of the priority program SPP 1991: TAXON-OMICS, 447176041). NJF was supported by an Erasmus+ traineeship grant.

References

Antonelli A, Kissling WD, Flantua SGA, Bermúdez MA, Mulch A, Muellner-Riehl AN, Kreft H, Linder HP, Badgley C, Fjeldså J, Fritz SA, Rahbek C, Herman F, Hooghiemstra H, Hoorn C (2018) Geological and climatic influences on mountain biodiversity. *Nature Geoscience* 11: 718–725. <https://doi.org/10.1038/s41561-018-0236-z>

Audacity Team (2014) Audacity(R): Free Audio Editor and Recorder. Version 2.1.0. <https://www.audacityteam.org> [accessed 30 June 2025].

Bandelt HJ, Forster P, Röhl A (1999) Median-joining networks for inferring intraspecific phylogenies. *Molecular Biology and Evolution* 16: 37–48. <https://doi.org/10.1093/oxfordjournals.molbev.a026036>

Belluardo F, Scherz MD, Santos B, Andreone F, Antonelli A, Glaw F, Muñoz-Pajares J, Randrianirina JE, Raselimanana AP, Vences M, Crottini A (2022) Molecular taxonomic identification and species-level phylogeny of the narrow-mouthed frogs of the genus *Rhombophryne* (Anura: Microhylidae: Cophylinae) from Madagascar. *Systematics and Biodiversity* 20: 1–13. <https://doi.org/10.1080/14772000.2022.2039320>

Bletz MC, Scherz MD, Rakotoarison A, Lehtinen R, Glaw F, Vences M (2018) Stumbling upon a new frog species of *Guibemantis* (Anura: Mantellidae) on top of the Marojejy Massif in northern Madagascar. *Copeia* 106: 255–263. <https://doi.org/10.1643/CH-17-655>

Brown JL, Cameron A, Yoder AD, Vences M (2014) A necessarily complex model to explain the biogeography of the amphibians and reptiles of Madagascar. *Nature Communications* 5: 5046. <https://doi.org/10.1038/ncomms6046>

Brown JL, Sillero N, Glaw F, Bora P, Vieites DR, Vences M (2016) Spatial biodiversity patterns of Madagascar's amphibians and reptiles. *PLoS One* 11: e0144076. <https://doi.org/10.1371/journal.pone.0144076>

Brown KA, Parks KE, Bethell CA, Johnson SE, Mulligan M (2015) Predicting plant diversity patterns in Madagascar: Understanding the effects of climate and land cover change in a biodiversity hotspot. *PLoS One* 10: e0122721. <https://doi.org/10.1371/journal.pone.0122721>

Bruford MW, Hanotte O, Brookfield JFY, Burke T (1992) Single-locus and multilocus DNA fingerprint. In: Hoelzel AR (Ed.) *Molecular Genetic Analysis of Populations: A Practical Approach*. IRL Press, Oxford, 225–270.

Cucciniello C, Melluso L, Morra V, Storey M, Rocco I, Francoisi L, Grifa C, Petrone CM, Vincent M (2011) New ^{40}Ar – ^{39}Ar ages and petrogenesis of the Massif d'Ambre volcano, northern Madagascar

Volcanism and Evolution of the African Lithosphere 478: 257–281. <https://doi.org/10.1130/9780813724782>

Darriba D, Taboada GL, Doallo R, Posada D (2012) jModelTest 2: More models, new heuristics and parallel computing. *Nature Methods* 9: 772. <https://doi.org/10.1038/nmeth.2109>

de Wit MJ (2003) Madagascar: Heads it's a continent, tails it's an island. *Annual Review of Earth and Planetary Sciences* 31: 213–248. <https://doi.org/10.1146/annurev.earth.31.100901.141337>

Donné Z, Rasoloniaina M, Djaovagnono HC, Kall B, Rabesiranana N, Rajaobelison J (2021) Study of water radioactivity transfer from telluric origin in the Amber Mountain, Antsiranana, Madagascar. *Scientific African* 13: e00902. <https://doi.org/10.1016/j.sciaf.2021.e00902>

Edler D, Klein J, Antonelli A, Silvestro D (2021) raxmlGUI 2.0: A graphical interface and toolkit for phylogenetic analyses using RAxML. *Methods in Ecology and Evolution* 12: 373–377. <https://doi.org/10.1111/2041-210X.13512>

Eiserhardt WL, Svenning J-C, Baker WJ, Couvreur TLP, Balslev H (2013) Dispersal and niche evolution jointly shape the geographic turnover of phylogenetic clades across continents. *Scientific Reports* 3: 1164. <https://doi.org/10.1038/srep01164>

Everson KM, Jansa SA, Goodman SM, Olson LE (2020) Montane regions shape patterns of diversification in small mammals and reptiles from Madagascar's moist evergreen forest. *Journal of Biogeography* 47: 2059–2072. <https://doi.org/10.1111/jbi.13945>

Flantua SGA, Hooghiemstra H (2018) Historical connectivity and mountain biodiversity. In: Hoorn C, Perrigo AL, Antonelli A (Eds) *Mountains, Climate and Biodiversity*. John Wiley & Sons, Hoboken NJ, 171–185.

Flantua SGA, O'Dea A, Onstein RE, Giraldo C, Hooghiemstra H (2019) The flickering connectivity system of the north Andean páramos. *Journal of Biogeography* 46: 1808–1825. <https://doi.org/10.1111/jbi.13607>

Flantua SGA, Payne D, Borregaard MK, Beierkuhnlein C, Steinbauer MJ, Dullinger S, Essl F, Irl SDH, Kienle D, Kreft H, Lenzner B, Norder SJ, Rijssdijk KF, Rumpf SB, Weigelt P, Field R (2020) Snapshot isolation and isolation history challenge the analogy between mountains and islands used to understand endemism. *Global Ecology and Biogeography* 29: 1651–1673. <https://doi.org/10.1111/geb.13155>

Frost DR (2025) *Amphibian Species of the World: An Online Reference*. Version 6.1. American Museum of Natural History, New York, NY, <https://amphibiansoftheworld.amnh.org> [accessed 29 July 2025].

Ganzhorn JU, Lowry PP, Schatz GE, Sommer S (2001) The biodiversity of Madagascar: One of the world's hottest hotspots on its way out. *Oryx* 35: 346–348. <https://doi.org/10.1046/j.1365-3008.2001.00201.x>

García-Rodríguez A, Martínez PA, Oliveira BF, Velasco JA, Pyron RA, Costa GC (2021) Amphibian speciation rates support a general role of mountains as biodiversity pumps. *American Naturalist* 198: E68–E79. <https://doi.org/10.1086/715500>

Gautier L, Tahinarivony JA, Ranirison P, Wohlhauser S (2018) Végétation/vegetation. In: Goodman SM, Raherilalao MJ, Wohlhauser S (Eds) *Les aires protégées terrestres de Madagascar: Leur histoire, description et biote/ The Terrestrial Protected Areas of Madagascar: Their History, Description, and Biota*. Association Vahatra, Antananarivo, 207–242.

Gehring P-S, Siarabi S, Scherz MD, Ratoavina FM, Rakotoarison A, Glaw F, Vences M (2018) Genetic differentiation and species status of the large-bodied leaf-tailed geckos *Uroplatus fimbriatus* and *U. giganteus*. *Salamandra* 54: 132–146.

Glaw F, Crottini A, Rakotoarison A, Scherz MD, Vences M (2022) Diversity and exploration of the Malagasy amphibian fauna. In: Goodman SM (Ed.) *The New Natural History of Madagascar*. Princeton University Press, Princeton, NJ, 1305–1322.

Glaw F, Köhler J, Vences M (2011) New species of *Gephyromantis* from Marojejy National Park, northeast Madagascar. *Journal of Herpetology* 45: 155–160. <https://doi.org/10.1670/10-058.1>

Glaw F, Köhler J, Vences M (2012) A tiny new species of *Platypelis* from the Marojejy National Park in northeastern Madagascar (Amphibia: Microhylidae). *European Journal of Taxonomy* 9: 1–9. <https://doi.org/10.5852/ejt.2012.9>

Goodenough KM, Thomas RJ, De Waele B, Key RM, Schofield DI, Bauer W, Tucker RD, Rafahatelo JM, Rabarimanana M, Ralison AV, Randriamananjara T (2010) Post-collisional magmatism in the central East African Orogen: The Maevanaro Suite of north Madagascar. *Lithos* 116: 18–34. <https://doi.org/10.1016/j.lithos.2009.12.005>

Goodman SM, Raherilalao MJ, Wohlhauser S (Eds) (2018) *Les Aires Protégées Terrestres de Madagascar: Leur Histoire, Description et Biote/The Terrestrial Protected Areas of Madagascar: Their History, Description, and Biota*. Vol. II: Northern and Eastern Madagascar. Vol. Association Vahatra, Antananarivo, 806 pp.

Graham MR, Flint WD, Powell AM, Fet V, Pauley TK (2023) Phylogeny of the cow knob salamander (*Plethodon punctatus* Highton): Populations on isolated Appalachian mountaintops are disjunct but not divergent. *Frontiers in Amphibian and Reptile Science* 1: 1175492. <https://doi.org/10.3389/famrs.2023.1175492>

Hall JP (2005) Montane speciation patterns in *Ithomiola* butterflies (Lepidoptera: Riodinidae): Are they consistently moving up in the world? *Proceedings of the Royal Society B* 272: 2457–2466. <https://doi.org/10.1098/rspb.2005.3254>

Hazzi NA, Wood HM (2025) Madagascar speciation on mountains: Pleistocene glaciation cycles promote genetic divergence, secondary contact, and morphological diversification in sympatric lineages of the pelican spider *Eriauchenus workmani* (Archaeidae). *Molecular Ecology*: e70007. <https://doi.org/10.1111/mec.70007>

Hending D, Sgarlata GM, Le Pors B, Rasolondraibe E, Jan F, Rakotonanahary AN, Ralantoharjaona TN, Debilois S, Andrianiaina A, Cotton S, Rasoloharjaona S, Zaonarivel JR, Andriaholinirina NV, Chikhi L, Salmona J (2020) Distribution and conservation status of the endangered Montagne d'Ambre fork-marked lemur (*Phaner electromontis*). *Journal of Mammalogy* 101: 1049–1060. <https://doi.org/10.1093/jmammal/gyaa065>

Hofmann S, Stöck M, Zheng Y, Ficetola FG, Li J-T, Scheidt U, Schmidt J (2017) Molecular phylogenies indicate a paleo-Tibetan origin of Himalayan lazy toads (*Scutiger*). *Scientific Reports* 7: 3308. <https://doi.org/10.1038/s41598-017-03395-4>

Katoh K, Rozewicki J, Yamada KD (2019) MAFFT online service: Multiple sequence alignment, interactive sequence choice and visualization. *Briefings in Bioinformatics* 20: 1160–1166. <https://doi.org/10.1093/bib/bbx108>

Knox EB (2004) Adaptive radiation of African montane plants. In: Dieckmann U, Doebeli M, Metz JA, Tautz D (Eds) *Adaptive Speciation*. Cambridge University Press, Cambridge, 345–361.

Köhler J, Jansen M, Rodriguez A, Kok PJR, Toledo LF, Emmrich M, Glaw F, Haddad CFB, Rödel M-O, Vences M (2017) The use of bioacoustics in anuran taxonomy: Theory, terminology, methods and recommendations for best practice. *Zootaxa* 4251: 1–124. <https://doi.org/10.11646/zootaxa.4251.1.1>

Lei F, Qu Y, Song G, Alström P, Fjeldså J (2015) The potential drivers in forming avian biodiversity hotspots in the East Himalaya Mountains of Southwest China. *Integrative Zoology* 10: 171–181. <https://doi.org/10.1111/1749-4877.12121>

Liu Y, Wang Y, Willett SD, Zimmermann NE, Pellissier L (2024) Escarpment evolution drives the diversification of the Madagascar flora. *Science* 383: 653–658. <https://doi.org/10.1126/science.adi0833>

Mayr E (1942) Systematics and the Origin of Species from the Viewpoint of a Zoologist. Columbia University Press, New York, NY, 334 pp.

Mohan AV, Gehring P-S, Scherz MD, Glaw F, Ratsoavina FM, Vences M (2019) Comparative phylogeography and patterns of deep genetic differentiation of two gecko species, *Paroedura gracilis* and *Phelsuma guttata*, across north-eastern Madagascar. *Salamandra* 55: 211–220.

Muellner-Riehl AN (2019) Mountains as evolutionary arenas: Patterns, emerging approaches, paradigm shifts, and their implications for plant phylogeographic research in the Tibeto-Himalayan region. *Frontiers in Plant Science* 10: 195. <https://doi.org/10.3389/fpls.2019.00195>

Muellner-Riehl AN, Schnitzler J, Kissling WD, Mosbrugger V, Rijksdijk KF, Seijmonsbergen AC, Versteegh H, Favre A (2019) Origins of global mountain plant biodiversity: Testing the ‘mountain-geobiodiversity hypothesis’. *Journal of Biogeography* 46: 2826–2838. <https://doi.org/10.1111/jbi.13715>

Nosil P (2012) Ecological Speciation. Oxford University Press, Oxford, 274 pp.

Oliver PM, Iannella A, Richards SJ, Lee MSY (2017) Mountain colonisation, miniaturisation and ecological evolution in a radiation of direct-developing New Guinea frogs (*Choerophryne*, Microhylidae). *PeerJ* 5: e3077. <https://doi.org/10.7717/peerj.3077>

Ortiz-Barrientos D, Grealy A, Nosil P (2009) The genetics and ecology of reinforcement. *Annals of the New York Academy of Sciences* 1168: 156–182. <https://doi.org/10.1111/j.1749-6632.2009.04919.x>

Phyletica Lab (2024) SPRI Bead DNA Extraction Protocol. <https://web.archive.org/web/20240525204441/https://phyletica.org/lab-protocols/extraction-spri.html> [accessed 30 June 2025].

R Core Team (2024) R: A Language and Environment for Statistical Computing. R Foundation for Statistical Computing, Vienna. <http://www.R-project.org> [accessed 30 June 2025].

Rabearivony J, Rasamolaina M, Raveloson J, Rakotomanana H, Raselimanana AP, Raminosoa NR, Zaonarivelo JR (2015) Roles of a forest corridor between Marojejy, Anjanaharibe-Sud and Tsaratanana protected areas, northern Madagascar, in maintaining endemic and threatened Malagasy taxa. *Madagascar Conservation & Development* 10: 85–92. <https://doi.org/10.4314/mcd.v10i2.7>

Rahbek C, Borregaard MK, Antonelli A, Colwell RK, Holt BK, Nogues-Bravo D, Rasmussen CMØ, Richardson K, Rosing MT, Whittaker RJ, Fjeldså J (2019) Building mountain biodiversity: Geological and evolutionary processes. *Science* 365: 1114–1119. <https://doi.org/10.1126/science.aax0151>

Rakotoarimalala F, Raselimanana AP (2023) Aperçu global de la tendance de la structure de la communauté herpétologique le long du gradient altitudinal du versant Est du Parc National de Marojejy au cours de ces 25 dernières années. *Malagasy Nature* 17: 165–186.

Rakotoarison A, Glaw F, Rasolontjatovo SM, Razafindraibe JH, Vences M, Scherz MD (2022) Discovery of frogs of the *Stumpffia hara* species group (Microhylidae, Cophylinae) on Montagne d’Ambre in northern Madagascar, with description of a new species. *Evolutionary Systematics* 6: 21–33. <https://doi.org/10.3897/evolsyst.6.76382>

Rakotoarison A, Scherz MD, Bletz MC, Razafindraibe JH, Glaw F, Vences M (2019a) Description of the lucky *Cophyla* (Microhylidae, Cophylinae), a new arboreal frog from Marojejy National Park in north-eastern Madagascar. *Zootaxa* 4651: 271–288. <https://doi.org/10.11646/zootaxa.4651.2.4>

Rakotoarison A, Scherz MD, Bletz MC, Razafindraibe JH, Glaw F, Vences M (2019b) Diversity, elevational variation, and phylogenetic origin of stump-toed frogs (Microhylidae: Cophylinae: *Stumpffia*) on the Marojejy massif, northern Madagascar. *Salamandra* 55: 115–123.

Rakotoarison A, Scherz MD, Glaw F, Köhler J, Andreone F, Franzen M, Glos J, Hawlitschek O, Jono T, Mori A, Ndriantsoa SH, Raminosoa Rasoamampionona N, Riemann JC, Rödel M-O, Rosa GM, Vieites DR, Crottini A, Vences M (2017) Describing the smaller majority: Integrative taxonomy reveals twenty-six new species of tiny microhylid frogs (genus *Stumpffia*) from Madagascar. *Vertebrate Zoology* 67: 271–298. <https://doi.org/10.3897/vz.67.e31595>

Rakotomalala D, Raselimanana AP (2003) Les amphibiens et reptiles des massifs de Marojejy, d’Anjanaharibe-Sud et du couloir forestier de Betaolana. In: Goodman SM, Wilémé L (Eds) Nouveaux résultats d’inventaires biologiques faisant référence à l’altitude dans la région des massifs montagneux de Marojejy et d’Anjanaharibe-Sud. Centre d’Information et de Documentation Scientifique et Technique, Antananarivo, 146–202.

Rambaut A (2018) FigTree. Version 1.4.4. <https://github.com/rambaut/figtree/releases> [accessed 30 June 2025].

Rancilhac L, Bruy T, Scherz MD, Pereira EA, Preick M, Straube N, Lyra M, Ohler A, Streicher JW, Andreone F, Crottini A, Hutter CR, Randrianantoandro JC, Rakotoarison A, Glaw F, Hofreiter M, Vences M (2020) Target-enriched DNA sequencing from historical type material enables a partial revision of the Madagascar giant stream frogs (genus *Mantidactylus*). *Journal of Natural History* 54: 87–118. <https://doi.org/10.1080/00222933.2020.1748243>

Raselimanana AP, Raxworthy CJ, Nussbaum RA (2000) Herpetofaunal species diversity and elevational distribution within the Parc National de Marojejy, Madagascar. *Fieldiana Zoology (New Series)* 97: 157–174.

Rasolontjatovo SM, Scherz MD, Rakotoarison A, Glos J, Raselimanana AP, Vences M (2020) Field body temperatures in the rainforest frog *Mantidactylus (Brygoomantis) bellyi* from northern Madagascar: Variance and predictors. *Malagasy Nature* 14: 57–68.

Rasolontjatovo SM, Scherz MD, Schmidt R, Glos J, Rakotoarison A, Raselimanana AP, Vences M (2022) Population diversification in the frog *Mantidactylus bellyi* on an isolated massif in northern Madagascar: Genetic, morphological, bioacoustic and ecological evidence. *PLoS One* 17: e0263764. <https://doi.org/10.1371/journal.pone.0263764>

Ratsoavina FM, Raselimanana AP, Scherz MD, Rakotoarison A, Glaw F, Vences M (2019) Finaritra! A new leaf-tailed gecko (*Uroplatus*) species from Marojejy National Park in north-eastern Madagascar. *Zootaxa* 4545: 563–577. <https://doi.org/10.11646/zootaxa.4545.4.7>

Ronquist F, Teslenko M, van der Mark P, Ayres DL, Darling A, Höhna S, Larget B, Liu L, Suchard MA, Huelsenbeck JP (2012) MR-BAYES 3.2: Efficient Bayesian phylogenetic inference and model selection across a large model space. *Systematic Biology* 61: 539–542. <https://doi.org/10.1093/sysbio/sys029>

RStudio Team (2019) RStudio: Integrated Development for R. RStudio, Boston, MA. <http://www.rstudio.com> [accessed 30 June 2025].

Scherz MD, Crottini A, Rakotoarison A (2022) Microhylidae: Cophylinae, microhylid frogs. In: Goodman SM (Ed.) The New Nat-

ural History of Madagascar. Princeton University Press, Princeton, NJ, 1382–1390.

Scherz MD, Köhler J, Rakotoarison A, Glaw F, Vences M (2019) A new dwarf chameleon, genus *Brookesia*, from the Marojejy massif in northern Madagascar. *Zoosystematics and Evolution* 95: 95–106. <https://doi.org/10.3897/zse.95.32818>

Scherz MD, Razafindraibe JH, Rakotoarison A, Bletz MC, Glaw F, Vences M (2017) Yet another small brown frog from high altitude on the Marojejy Massif, northeastern Madagascar. *Zootaxa* 4347: 572–582. <https://doi.org/10.11646/zootaxa.4347.3.9>

Scherz MD, Ruthensteiner B, Vences M, Glaw F (2014) A new microhylid frog, genus *Rhombophryne*, from northeastern Madagascar, and a re-description of *R. serratopalpebrosa* using micro-computed tomography. *Zootaxa* 3860: 547–560. <https://doi.org/10.11646/zootaxa.3860.6.3>

Scherz MD, Schmidt R, Brown JL, Glos J, Lattenkamp EZ, Rakotomalala Z, Rakotoarison A, Rakotonindrina RT, Randriamalala O, Raselimanana AP, Rasoloniato SM, Ratsoavina FM, Razafindraibe JH, Glaw F, Vences M (2023) Repeated divergence of amphibians and reptiles across an elevational gradient in northern Madagascar. *Ecology and Evolution* 13: e9914. <https://doi.org/10.1002/ece3.9914>

Scherz MD, Vences M, Rakotoarison A, Andreone F, Köhler J, Glaw F, Crottini A (2016) Reconciling molecular phylogeny, morphological divergence and classification of Madagascan narrow-mouthed frogs (Amphibia: Microhylidae). *Molecular Phylogenetics and Evolution* 100: 372–381. <https://doi.org/10.1016/j.ympev.2016.04.019>

Steinbauer MJ, Field R, Grytnes JA, Trigas P, Ah-Peng C, Attorre F, Birks HJB, Borges PAV, Cardoso P, Chou C-H, De Sanctis M, de Sequeira MM, Duarte MC, Elias RB, Fernández-Palacios JM, Gabriel R, Gereau RE, Gillespie RG, Greimler J, Harter DEV, Huang T-J, Irl SDH, Jeanmonod D, Jentsch A, Jump AS, Kueffer C, Nogué S, Otto R, Price J, Romeiras MM, Strasberg D, Stuessy T, Svenning J-C, Vetaas OR, Beierkuhnlein C (2016) Topography-driven isolation, speciation and a global increase of endemism with elevation. *Global Ecology and Biogeography* 25: 1097–1107. <https://doi.org/10.1111/geb.12469>

Stephens M, Smith NJ, Donnelly P (2001) A new statistical method for haplotype reconstruction from population data. *American Journal of Human Genetics* 68: 978–989. <https://doi.org/10.1086/319501>

Tu N, Yang M, Liang D, Zhang P (2018) A large-scale phylogeny of Microhylidae inferred from a combined dataset of 121 genes and 427 taxa. *Molecular Phylogenetics and Evolution* 126: 85–91. <https://doi.org/10.1016/j.ympev.2018.03.036>

Vences M, Gehara MC, Köhler J, Glaw G (2012) Description of a new Malagasy treefrog (*Boophis*) occurring syntopically with its sister species, and a plea for studies on non-allopatric speciation in tropical amphibians. *Amphibia-Reptilia* 33: 503–520. <https://doi.org/10.1163/15685381-00002856>

Vences M, Köhler J, Andreone F, Craul A-K, Crottini A, du Preez L, Preick M, Rancilhac L, Rödel M-O, Scherz MD, Streicher JW, Hofreiter M, Glaw F (2021a) Target-enriched DNA sequencing clarifies the identity of name-bearing types of the *Gephyromantis plicifer* complex and reveals a new species of mantellid frog from Madagascar (Amphibia, Anura). *Spixiana* 44: 175–202.

Vences M, Lyra ML, Perl BRG, Bletz MC, Stankovic D, Geffers R, Haddad CFB, Steinfartz S, Martins Lopes C, Jarek M, Bhuju S (2016) Freshwater vertebrate metabarcoding on Illumina platforms using double-indexed primers of the mitochondrial 16S rRNA gene. *Conservation Genet Resources* 8: 1–5. <https://doi.org/10.1007/s12686-016-0550-y>

Vences M, Miralles A, Brouillet S, Ducasse J, Fedosov A, Kharchev V, Kostadinov I, Kumari S, Patmanidis S, Scherz MD, Puillandre N, Renner SS (2021b) iTaxoTools 0.1: Kickstarting a specimen-based software toolkit for taxonomists. *Megataxa* 6: 77–92. <https://doi.org/10.11646/megataxa.6.2.1>

Vences M, Multzsch M, Gippner S, Miralles A, Crottini A, Gehring P-S, Rakotoarison A, Ratsoavina FM, Glaw F, Scherz MD (2022) Integrative revision of the *Lygodactylus madagascariensis* group reveals an unexpected diversity of little brown geckos in Madagascar's rainforest. *Zootaxa* 5179: 1–61. <https://doi.org/10.11646/zootaxa.5179.1.1>

Vences M, Patmanidis S, Schmidt J-C, Matschiner M, Miralles A, Renner SS (2024) Hapsolutely: A user-friendly tool integrating haplotype phasing, network construction, and haploweb calculation. *Bioinformatics Advances* 4: vbae083. <https://doi.org/10.1093/bioadv/vbae083>

Vieites DR, Wollenberg KC, Andreone F, Köhler J, Glaw F, Vences M (2009) Vast underestimation of Madagascar's biodiversity evidenced by an integrative amphibian inventory. *Proceedings of the National Academy of Sciences of the USA* 106: 8267–8272. <https://doi.org/10.1073/pnas.0810821106>

Vences M, Wollenberg KC, Vieites DR, Lees DC (2009) Madagascar as a model region of species diversification. *Trends in Ecology and Evolution* 24: 456–465. <https://doi.org/10.1016/j.tree.2009.03.011>

Wesener T, Raupach MJ, Decker P (2011) Mountain refugia play a role in soil arthropod speciation on madagascar: A case study of the endemic giant fire-millipede genus *Aphistogoniulus*. *PLoS ONE* 6: e28035. <https://doi.org/10.1371/journal.pone.0028035>

Wickham H (2016) *ggplot2: Elegant Graphics for Data Analysis*. Springer-Verlag, New York NY, 260 pp.

Wickham H, Averick M, Bryan J, Chang W, D'Agostino McGowan L, François R, Gromelund G, Hayes A, Henry L, Hester J, Kuhn M, Pedersen TL, Miller E, Milton Bache S, Müller K, Ooms J, Robinson D, Seidel DP, Spinu V, Takahashi K, Vaughan D, Wilke C, Woo K, Yutani H (2019) Welcome to the Tidyverse. *Journal of Open Source Software* 4: 1686. <https://doi.org/10.21105/joss.01686>

Wilmé L, Goodman SM, Ganzhorn JU (2006) Biogeographic evolution of Madagascar's microendemic biota. *Science* 312: 1063–1065. <https://doi.org/10.1126/science.1122806>

Wollenberg KC, Vieites DR, van der Meijden A, Glaw F, Cannatella DC, Vences M (2008) Patterns of endemism and species richness in Malagasy cophyline frogs support a key role of mountainous areas for speciation. *Evolution* 62: 1890–1907. <https://doi.org/10.1111/j.1558-5646.2008.00420.x>

Wollenberg Valero KC (2015) Evidence for an intrinsic factor promoting landscape genetic divergence in Madagascan leaf-litter frogs. *Frontiers in Genetics* 6: 1–7. <https://doi.org/10.3389/fgene.2015.00155>

Appendix

Bioacoustic key to *Stumpffia* species of Montagne d'Ambre

This dichotomous key is designed to be used during field-work and works exclusively for advertisement calls of *Stumpffia* recorded on Montagne d'Ambre, except for *S. sp. aff. angeluci* due to the lack of bioacoustic data. Dominant frequencies can be obtained from various modern smart phone applications and the number of calls per ten seconds can easily be counted. Depending on the motivation of the calling male, the time interval for counting should be chosen as large as possible, given it is calling regularly. Subsequently, calls per ten seconds can be calculated. Note that this key only applies to reasonably

motivated individuals calling on Montagne d'Ambre and may else fail.

To distinguish in step seven between *S. angeluci* and the remaining species *S. maledicta* and *S. bishopi*, the recording of the call duration is necessary. Note, that already recorded specimens of *S. angeluci* showed very distant call durations compared to *S. maledicta* and *S. bishopi* (Fig. 8H; Table 1). Furthermore, the final distinction between *S. maledicta* and *S. bishopi* is difficult due to large overlap between their call durations, dominant frequencies, and calls per ten seconds.

1a) Dominant frequency above 3700 Hz	2
1b) Dominant frequency below 3700 Hz	<i>S. megsoni</i>
2a) Dominant frequency above 5550 Hz	3
2b) Dominant frequency below 5550 Hz	4
3a) More than 2.5 calls per 10 s	<i>S. mamitika</i>
3b) Less than 2.5 calls per 10 s	<i>S. madagascariensis</i>
4a) Dominant frequency above 4600 Hz	<i>S. huwei</i>
4b) Dominant frequency mostly below 4600 Hz	5
5a) Dominant frequency below 4030 Hz	6
5b) Dominant frequency above 4030 Hz	7
6a) More than 2.3 calls per 10 s	<i>S. madagascariensis</i>
6b) Less than 2.3 calls per 10 s	<i>S. bishopi</i>
7a) Call duration longer than 150 ms	<i>S. angeluci</i>
7b) Call duration shorter than 150 ms	8
8a) Dominant frequency mostly above 4100 Hz	<i>S. maledicta</i>
8b) Dominant frequency mostly below 4100 Hz, less than 2.3 calls per 10 s	<i>S. bishopi</i>

Supplementary Material 1

Figures S1–S5

Authors: Fleck NJ, Petzold A, Rakotoarison A, Vences M, Scherz MD (2026)

Data type: .pdf

Explanation notes: **Figure S1.** Maximum likelihood phylogeny of *Stumpffia* based on Alignment B (5' 16S). Node labels are given as bootstrap values, not displayed when below 50. — **Figure S2.** Maximum likelihood phylogeny of *Stumpffia* based on Alignment A (16S 3'). Node labels are given as bootstrap values, not displayed when below 50. — **Figure S3.** Bayesian phylogeny of *Stumpffia* based on the concatenated Alignment C (3'+5' 16S). Node labels are given as posterior probabilities. Bolded species and specimens indicate occurrence on Montagne d'Ambre. — **Figure S4.** Maximum likelihood phylogeny of *Stumpffia* based on Alignment B (16S 5'). Only members of Clade A according to Rakotoarison et al. (2017) are shown; their position in the overall *Stumpffia* phylogeny is indicated by a grey rectangle. Specimens from Montagne d'Ambre are bolded. Node labels are given as bootstrap values, not displayed when below 50. — **Figure S5.** Third and fourth principal components of our principal component analysis (PCA) of morphometric data on *Stumpffia* that occur on Montagne d'Ambre (raw data in Table S5).

Copyright notice: This dataset is made available under the Open Database License (<http://opendatacommons.org/licenses/odbl/1.0>). The Open Database License (ODbL) is a license agreement intended to allow users to freely share, modify, and use this dataset while maintaining this same freedom for others, provided that the original source and author(s) are credited.

Link: <https://doi.org/10.3897/vz.76.e166419.suppl1>

Supplementary Material 2

Tables S1–S7

Authors: Fleck NJ, Petzold A, Rakotoarison A, Vences M, Scherz MD (2026)

Data type: .zip

Explanation notes: **Table S1.** Approximate fragment sizes (bp), primer sequences and thermal cycling profiles used for the amplification of DNA fragments. Thermal cycling schemes start with temperature (in °C) of each step, followed by the time in seconds between parentheses; cycling repetitions are indicated within brackets. Direction is given as “F” for forward and “R” for reverse primer. — **Table S2.** GenBank accession numbers for all newly generated sequences used in Alignments A, B, and C. — **Table S3.** Pairwise uncorrected p-distances of the 16S 5' phylogeny calculated from Alignment B, given as ‘mean (minimum – maximum)’ and in percent. — **Table S4.** Pairwise uncorrected p-distances of the 16S 3' phylogeny calculated from Alignment A, given as ‘mean (minimum – maximum)’ and in percent. — **Table S5.** Morphometric data from *Stumpffia* species occurring on Montagne d'Ambre. For abbreviations see ‘Material and methods’ section. ‘Mea’ is measurer (AR = A. Rakotoarison; NJF = N. J. Fleck). This data is an alignment of own measurements as well as data from Rakotoarison et al. (2017, 2022). Numbers are given in mm. — **Table S6.** Morphometric data from *Stumpffia* species occurring on Montagne d'Ambre. Specimens were collected on Montagne d'Ambre (‘d'Ambre’) or at a different location (‘not d'Ambre’). For abbreviations see Material and methods section. This data is a combination of our own measurements as well as data from Rakotoarison et al. (2017, 2022). Values are given in mm as ‘minimum – maximum (mean ± standard deviation, N = number of examined specimens)’. See Table S5 for our raw measurement data. — **Table S7.** Pairwise uncorrected p-distances of the concatenated 16S 3' and 5' phylogeny calculated from Alignment C, given as ‘mean (minimum – maximum)’ and in percent.

Copyright notice: This dataset is made available under the Open Database License (<http://opendatacommons.org/licenses/odbl/1.0>). The Open Database License (ODbL) is a license agreement intended to allow users to freely share, modify, and use this dataset while maintaining this same freedom for others, provided that the original source and author(s) are credited.

Link: <https://doi.org/10.3897/vz.76.e166419.suppl2>